The Thesis Committee for **Umid Azimov**
Certifies that this is the approved version of the following thesis:

Controlling Cracking in Precast Prestressed Concrete Panels

APPROVED BY
SUPERVISING COMMITTEE:

Richard E. Klingner, Supervisor

James O. Jirsa

Controlling Cracking in Precast Prestressed Concrete Panels

by

Umid Azimov, B.S.C.E.

Thesis

Presented to the Faculty of the Graduate School of

The University of Texas at Austin

in Partial Fulfillment

of the Requirements

for the Degree of

Master of Science in Engineering

The University of Texas at Austin

August, 2012

DEDICATION

To my family in Chust and Austin

To my daughter Sofiya

ACKNOWLEDGEMENTS

I would like to express my deepest appreciation to my advisors, Dr. Richard E. Klingner, Dr. James O. Jirsa and Dr. Oguzhan Bayrak. I thank you all for providing guidance and support throughout this research study. Thank you for always being available and willing to provide assistance during the project and thesis. Thank you for teaching technical knowledge and professionalism, and for your invaluable advice in writing this thesis.

I am grateful for the financial support provided by Texas Department of Transportation for Research Study 0-6348.

I greatly appreciate the support and dedication of my research team members, Ki Yeon Kwon and Aaron P. Woods. I am also grateful for the hard work of Phil M. Ferguson Structural Engineering Laboratory technical staff (Andrew Valentine, Blake Stasney, Mike Watson, Dennis Fillip, Eric Schell and Barbara Howard) and my fellow students (Ali Abu-Yousef, Kerry Kreitman, Hossein Yousefpour).

Last but not least, I would like to thank my family in Chust (the Azimovs) and in Austin (the Gronbergs), and my wife Dildora for always providing moral support and encouragement all throughout my stay at the University of Texas at Austin.

August 1, 2012

ABSTRACT

Controlling Cracking in Precast Prestressed Concrete Panels

Umid Azimov, M.S.E.

The University of Texas at Austin, 2012

Supervisor: Richard E. Klingner

Precast, prestressed concrete panels (PCPs) have been widely used in Texas as stay-in-place formwork in bridge deck construction. Although PCPs are widely popular and extensively used, Texas is experiencing problems with collinear cracks (cracks along the strands) in panels. One reason for the formation of collinear cracks is thought to be the required level of initial prestress. Currently, PCPs are designed assuming a 45-ksi, lump-sum prestress loss. If the prestress losses are demonstrated to be lower than this value, this could justify the use of a lower initial prestress, probably resulting in fewer collinear cracks. For this purpose, 20 precast, prestressed panels were cast at two different plants. Half of those 20 panels were fabricated with the current TxDOT-required prestress of 16.1 kips per strand, and the other half were fabricated with a lower prestress of 14.4 kips per strand based on initially observed prestress losses of 25 ksi or less. Thirteen of those panels were instrumented with strain gages and monitored over their life time. Observed losses stabilized after five months, and are found to be about 24.4 ksi. Even with the reduced initial prestress, the remaining prestress in all panels exceeds the value now assumed by TxDOT for design.

TABLE OF CONTENTS

LIST OF TABLES

LIST OF FIGURES

CHAPTER 1
Introduction

1.1 OVERVIEW

Precast, prestressed concrete panels (PCPs) have been widely used in Texas as stay-in-place formwork in bridge deck construction. The use of PCPs has improved workers' safety, increased the speed of construction, and has proved to be a cost-efficient method for bridge construction. The Texas Department of Transportation (TxDOT) has developed highly standardized PCP construction details over many years, and has encouraged their use.

PCPs are fabricated at a precast yard as 4-in. thick panels, and typically measure 8 ft in the longitudinal and transverse directions. However, the longitudinal and transverse dimensions are adjusted according to girder spacing and span. The transverse direction of the panel is prestressed with 3/8-in. diameter, 7-wire strands. After the PCPs are fabricated and cured, they are transported to project site and lifted into place to span between girders. Once the PCPs are placed on girders and a 4-in. cast-in-place (CIP) topping is cast, as shown in Figure 1.1, the deck acts compositely.

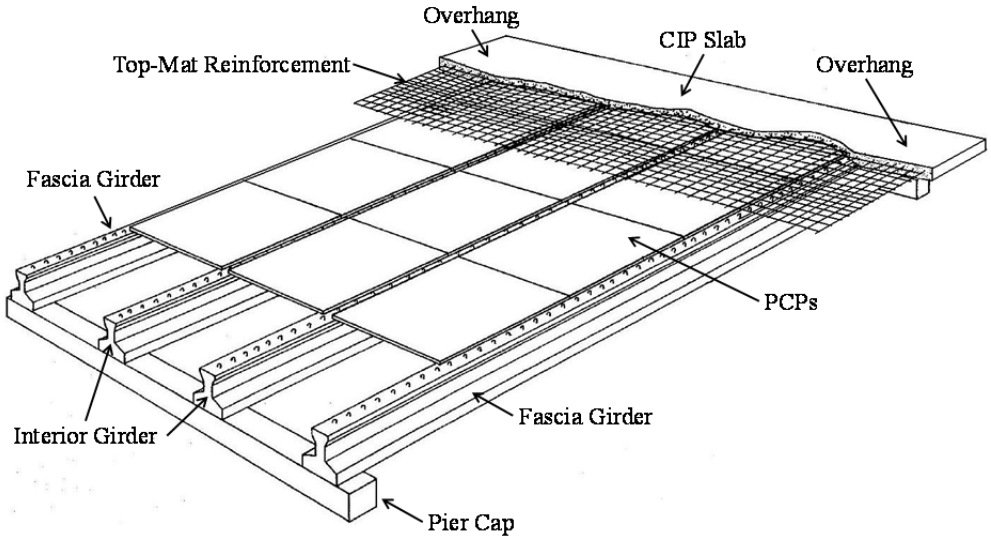

Figure 1.1 Typical PCP-CIP bridge deck system (Foster 2010, Buth et al. 1972)

Although PCPs are widely popular and extensively used in bridge deck construction, Texas is experiencing problems with collinear cracks (cracks along the strands) in panels. The cracked panels are rejected by inspectors because of the concerns over prestress loss, which can reduce panel stiffness and conceivably reduce performance life. One reason for the formation of collinear cracks is thought to be the required level of initial prestress. Currently, PCPs are designed assuming a 45-ksi, lump-sum prestress loss. If the prestress losses are demonstrated to be lower than this value, this could justify the use of a lower initial prestress, probably resulting in fewer collinear cracks. In an effort to reduce the rejection rates of precast panels and other bridge-deck related concerns, TxDOT sponsored Research Study 0-6348 ("Controlling Cracking in Prestressed Concrete Panels and Optimizing Bridge Deck Reinforcing Steel"). The main objective of this thesis is focused on experimentally determining the actual prestress losses in panels.

1.2 OBJECTIVES

The objectives of the portion of the Research Study 0-6348 related to controlling cracking in precast, prestressed concrete panels are the following:

1) Review the existing TxDOT precast, prestressed concrete panel (PCP) design to understand the underlying assumptions used in determining the prestress loss;

2) Experimentally determine the actual prestress losses experienced by panels;

3) Examine the possibility of reducing the initial prestress;

4) Examine to ensure that the final or effective prestress force remains unchanged if the reduced initial prestress force is applied;

5) Evaluate causes of PCP cracking and determine if improvements in construction techniques and materials could reduce PCP cracking;

6) Reduce the rate of rejected PCPs;

7) Reduce initial circumferential tensile stresses at release and consequently reduce the total tensile stresses;

8) Determine actual prestress losses in PCPs;

9) Recommend application of reduced initial prestress force;

10) Evaluate the effectiveness of additional edge reinforcement in panels to control the crack formation collinear to strands; and

11) Recommend new design alternatives as necessary.

Within the objectives of the Research Study 0-6348, the objectives of this thesis are:

1) Determine actual prestress losses in PCPs;
2) Demonstrate that actual prestress losses are less than the 45 ksi that is now assumed in design (45ksi);
3) Recommend new reduced initial prestress force;
4) Recommend new design alternatives as necessary.

1.3 SCOPE

This thesis is a continuation of work described in Foreman (2010). It deals with that portion of TxDOT Research Study 0-6348 related to controlling cracking in precast, prestressed panels. That work includes a thorough literature review, and describes laboratory experiments to measure prestress losses in panels and investigates the effectiveness of additional edge reinforcement on crack control. Using field-instrumented panels fabricated at two different precast plants, prestress losses were monitored over

time. Panels included those with currently approved details, and also a variant with additional transverse reinforcement at ends.

As a continuation of that research, this work includes additional literature review. The panels described in Foreman (2010) continue to be monitored for prestress losses. Based on recommendations of Foreman (2010), additional instrumented panels with reduced initial prestress force were fabricated at the same two plants, including the same variants in transverse reinforcement, and are monitored for prestress losses. Repair of cracks is not investigated. The researchers express no opinion on whether cracked panels should be accepted by TxDOT inspectors.

1.4 ORGANIZATION

The details of the work performed over the course of this research study are presented in the following chapters. Chapter 2 contains a literature review of the mechanism of and factors affecting panel cracking, and also a review of previous research on panels. Introduction to testing program, fabrication and monitoring of panels at Plant A and at Plant B are described in Chapter 3, Chapter 4 and Chapter 5, respectively. The test results from monitoring are presented and discussed in Chapter 6. Summary, conclusion and recommendations based on the experimental investigation performed during the study are provided in Chapter 7.

CHAPTER 2
Literature Review

2.1 INTRODUCTION

Precast, prestressed concrete panels (PCPs) span between bridge girders and act as stay-in-place forms for bridge deck cast-in-place concrete. Once the top deck is cast the PCPs act compositely to resist the applied loads. According to the TxDOT 0-6348 project statement, nearly 200,000 panels are rejected annually due to the cracking of panels collinear to the strands. This cracking generally develops due to a combination of tensile stresses at release, handling at precast yard, transportation to the job site, and handling at the job site (TxDOT 6348, 2010). Foreman (2010) conducted a thorough literature review on the development of PCPs, significance, causes and prevention of cracking in PCPs. In this chapter, that review is summarized and updated.

Cracking along the prestressing strands in panels can be explained by Tepfers' model for steel-concrete bond (Tepfers, 1975) and Hoyer's effect (Hoyer, 1939). As shown in Figure 2.1, axial forces in prestressing strands are resisted by inclined forces, acting inward from the concrete surrounding the strands (Tepfers, 1975). Corresponding inclined forces act outward from the strands against the concrete. The radial components of those forces produce circumferential tensile stresses in the concrete surrounding the strands. As the prestressing strands shorten elastically, they expand laterally due to Poisson effects, producing additional radial compressive forces in the concrete surrounding the strands, and additional circumferential tensile stresses in that concrete (Hoyer, 1939). Those circumferential tensile stresses are resisted by the tensile strength of the concrete around the strands. When that tensile strength is exceeded, cracks form in the surrounding concrete parallel to the strands (Benítez *et al.*, 2011). When those cracks propagate to the surface, they are referred to as "collinear cracks" (TxDOT 6348, 2010).

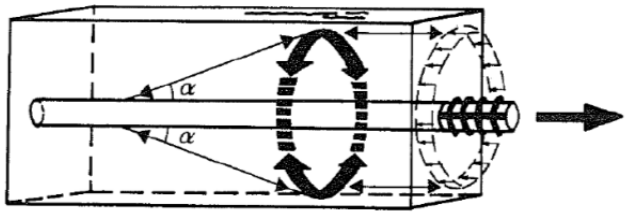

Figure 2.1 Schematic representation of how the radial components of the bond forces are balanced by tensile stress rings in the concrete in anchorage zone (Tepfers 1975).

Based on the 1988 PCI special report, the TxDOT standard specification presents two criteria for rejection of panels (Ross Associates, Inc., 1988; TxDOT, 2004):

1) Any crack extending to the reinforcing plane and running parallel and within 1 in. of a strand for at least 1/3 of the embedded strand length; or

2) Any transverse or diagonal crack, including corner cracks and breaks, intersecting at least two adjacent strands and extending to the reinforcing plane.

The main causes of longitudinal cracking are excessive prestress force, inadequate transverse reinforcement and improper release of prestressing strand (PCI, 2006; FIB, 2007). The first two causes are investigated and addressed in Foreman (2010) and in this research project. The third cause is normally avoided by Texas precasters by slowly torch-cutting the strands at release (Foreman, 2010).

Collinear cracking can be prevented by reducing the initial prestress force and by providing supplemental reinforcement at the edges of a panel perpendicular to the strands, separately or in combination (TxDOT 6348, 2010). Generally, the initial prestress force is set equal to the final desired prestress force plus the expected losses (Foreman, 2010). The primary sources of the expected prestress losses are elastic shortening of the concrete when the strands are released, creep and shrinkage of concrete, and relaxation of strands. In designing the PCPs, TxDOT uses a lump-sum estimate of 45 ksi for expected losses (TxDOT, 2001). However, based on panel testing and long-term monitoring, Foreman (2010) concluded that the estimate of 45 ksi for losses is conservative (high), and that a figure of 25 ksi would be more accurate.

Marti-Vargas *et al.* (2012) investigated the influence of concrete composition and different water/cement ratio on the bond behavior over the transfer length of prestressing strand. The researchers prepared test specimens with varying cement content and varying water/cement ratios. They found that bond stress decreases with increasing w/c ratio for same cement content. Decreasing bond stress corresponds to a longer transfer length. Additionally, for low cement factors (350 kg/m^3), the transfer length remained constant and there was negligible influence of w/c ratio.

Concrete expands and contracts with temperature changes, with a change in strain equal to the change in temperature multiplied by the coefficient of thermal expansion (CTE) (Jahangirnejad *et al.*, 2010). Because coarse aggregates constitute about 75% of the volume of concrete, they play a significant role in influencing the overall CTE of concrete (Naik *et al.*, 2011). To minimize thermal expansion and contraction of concrete, it is useful to include the CTE in the design process. Naik et al. examined the influence of types of aggregate on CTE of concrete. Gravel course aggregates were observed to have CTE values ranging from 9.1 to 10.7 microstrain/°C (Naik *et al.*, 2011). Emanuel *et al.* (1977) report values of 7.4 microstrain/°C for gravel aggregates and 6.3 microstrain/°C for limestone aggregates.

2.2 TxDOT Project 0-6348 (Foreman 2010)

The research of Foreman (2010) was part of this project. Foreman fabricated ten panels at two different precast panels in Texas to determine the actual prestress losses and the effectiveness of additional reinforcement at the edges to control cracks. Half of the panels were fabricated with the current TxDOT standard detailing, and the other half were modified to include additional reinforcement at the end edges. All the panels were designed according to TxDOT specification and had minimum specified 28-day compressive strength of 4,000 psi. Because each plant used locally available aggregates nearby the plant, the concrete mix contained either limestone coarse aggregate or river gravel, depending on the plant.

Average measured short-term prestress losses related to elastic shortening of concrete at release were 3.4 ksi, slightly lower than the AASHTO estimate of 5.0 ksi. Results from long-term monitoring of prestress losses were less than 25 ksi, as shown in Figure 2.2 (Note: only upper portion of the graph is shown). As it can be seen from that figure, AASHTO 2008 and TxDOT predictions overestimate the prestress losses by 40% and 80%, respectively. However, AASHTO 2004 equations appear more accurate in predicting losses in panels.

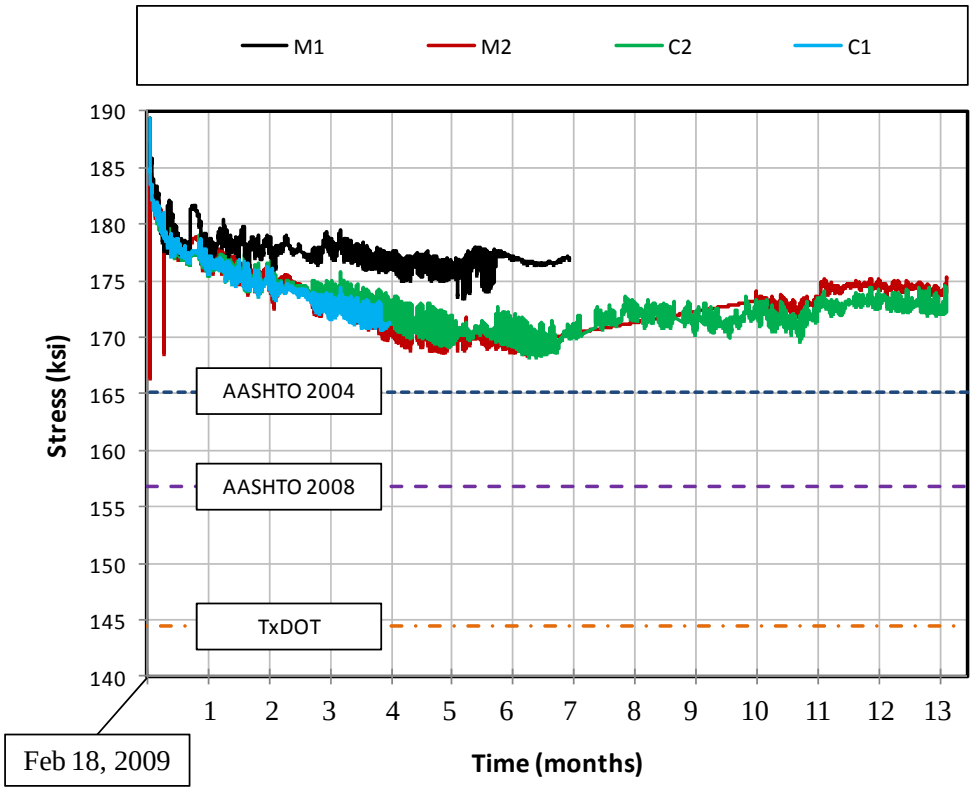

Figure 2.2 Long term stresses in panels cast at Plant A (M-specimens are modified, C-specimens are current TxDOT standard) (Foreman 2010)

A knife-edge test (Figure 2.3) was performed to investigate the relationship between and panel cracking and prestress loss, and also to compare the effectiveness of supplemental reinforcing bars in controlling collinear cracks.

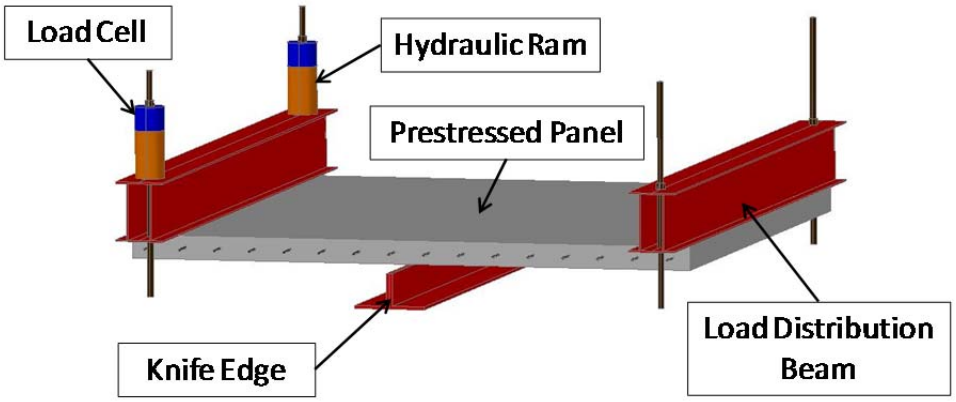

Figure 2.3 Knife-edge test specimen (Foreman 2010)

As the panels were bent over the knife edge, Foreman measured crack widths and counted the number of cracks. He observed that with additional transverse reinforcement at the edges, the crack widths decreased and the number of cracks increased. The loss of prestress was also observed to be very small, even for wide cracks. Until crack width reached 0.01 in. (a value noted by TxDOT inspectors in the field), strand slip was minimal. Foreman (2010) concludes that cracks of such width do not significantly affect the effective prestress.

2.3 SUMMARY

Precast, prestressed concrete panels (PCPs) have widely been used in Texas as stay-in-place forms in bridge deck construction. Over many years, TxDOT has improved the use of PCPs, and has developed standard details for them.

PCPs in Texas sometimes have collinear cracks along the strands, resulting in the rejection of about 200,000 panels each year. The main cause of this collinear cracking is the initial prestress force. That initial prestress can be reduced if more accurate prestress losses can be used in design. To date, only Foreman (2010) has specifically investigated prestress losses in panels. His work shows typical prestress losses of 25 ksi or less, much lower than the 45 ksi now assumed by TxDOT in designing the panels.

CHAPTER 3
Introduction to Testing Program

3.1 FIELD FABRICATION

As a continuation of the work described in Foreman (2010) and as a part of TxDOT Research Project 0-6348, an additional eight precast, prestressed concrete panels (4 modified, 4 current) were instrumented and fabricated at two different Texas plants, referred to here as Plant A and Plant B. After fabrication, the panels were transported and monitored continuously for long-term prestress losses at Ferguson Structural Engineering Laboratory.

3.1.1 Objectives of field fabrication and panel monitoring

The objective of fabricating and monitoring panels is to assess actual prestress losses. To confirm the findings of Foreman (2010), an additional eight panels were fabricated. The panels described in Foreman (2010) were fabricated in February, 2009 and 2010, and are referred to here as "Winter Panels." To observe possible differences in behavior associated with different mixtures used in different seasons, the eight additional panels were fabricated in July, 2010 and September, 2010, and are referred to here as "Summer Panels." The eight additional panels had lower initial prestress than those described by Foreman, with the objectives of examining whether prestress losses were consistent and whether reduced prestress would result in less collinear panel cracking.

3.1.2 General sequence of field fabrication and panel monitoring

1) Precast, prestressed panels were fabricated at two different Texas plants. The panel strands and reinforcement were instrumented with gauges and concrete was cast on the first day. After a day or two, the strands were released and the panels were stored in stacks at the precast yard.

2) Approximately two weeks after casting, the panels were transported to the Ferguson Structural Engineering Laboratory, and were stored in stacks of four outside the laboratory.

3) Each panel has been continuously monitored for prestress losses by analyzing the strain data acquired through an automated data acquisition system.

CHAPTER 4
Fabrication and Panel Monitoring at Plant A

4.1 FIELD FABRICATION

Four panels were instrumented and cast at Plant A on July 20th, 2010. The panels were fabricated with a reduced initial prestress of 169.4 ksi, less than the current TxDOT requirement of 189.4 ksi. Two of the four panels were provided with additional transverse reinforcement at each end, and are referred to here as Specimens M5 and M6. The other two panels conformed to current TxDOT requirements, and are referred to here as Specimens C6 and C7.

4.1.1 Panel Design

Prestressed concrete panels are designed according to the TxDOT Bridge Design Manual following the AASHTO Standard Specifications for Highway Bridges (TxDOT, 2001). These include a concrete mixture with a specified release strength f_{ci}' of 4000 psi and a minimum specified 28-day strength f_c' of 5000 psi. Each plant establishes its own mixture design to meet those requirements. Sections 4.1.1.1 and 4.1.1.2 discuss the panel reinforcement details and concrete mixture design used by Plant A, as well as the additional reinforcement added by researchers for this project.

4.1.1.1 Reinforcement

As shown in Figure 4.1, Plant A uses welded wire mesh for transverse reinforcement and ½-in. diameter prestressing strands at 6-in. spacing for longitudinal reinforcement. TxDOT standard details for prestressed concrete panel fabrication (Appendix A.1) offer several options for transverse reinforcement, including No. 3 bars at 6-in. spacing, 3/8-in. diameter prestressing strands at 4.5-in. spacing, ½-in. diameter prestressing strands at 6-in. spacing, and deformed welded-wire reinforcement providing

0.22 square inches per foot of panel width. Plant A uses D7.5 welded-wires mesh at a 4-in. spacing in transverse directions. The mesh is placed directly on top of the prestressing strands, and is tied at a few locations after the strands are fully stressed.

Figure 4.1 Welded wire mesh and strands in place at Plant A

Specimens M5 and M6 were provided with additional transverse reinforcing bars placed 1 in. from each end of the panels. As shown in Figure 4.2, one end of the panel has two additional No. 3 bars stacked vertically and separated by No. 5 bars. The other end has additional reinforcement because the welded-wire mesh was placed closer to the end as shown in Figure 4.3. This additional reinforcement was intended to control the width and growth of the cracks collinear to strands. The purpose of providing two different amounts of transverse reinforcement at the ends is to compare the effectiveness of different design alternatives.

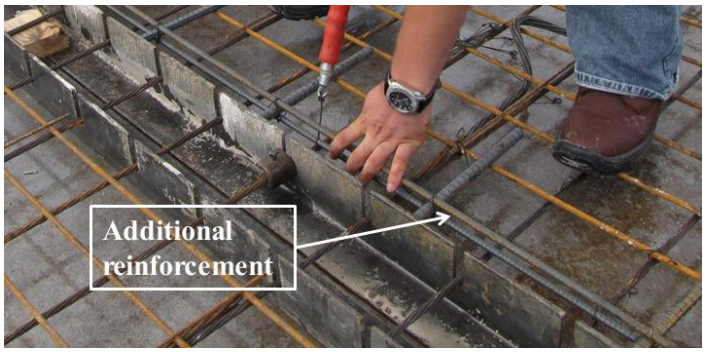

Figure 4.2 Two additional reinforcing bars at one end at Plant A

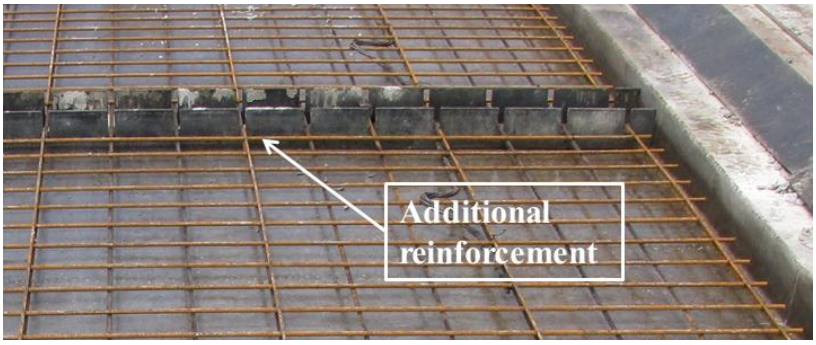

Figure 4.3 One additional reinforcing bar at one end at Plant A

4.1.1.2 Concrete Mixture Design

TxDOT Prestressed Concrete Panel Fabrication Details (Appendix A.1) indicate that all concrete for panels is to be Class H, with a specified release strength of 4000 psi and a specified minimum 28-day strength of 5000 psi. Plant A produces a mixture with a target release strength of 5000 psi and a target minimum 28-day strength of 9000 psi. Plant A uses crushed limestone aggregate for the concrete mixture. As summarized in Table 4.1, tests performed at Ferguson Laboratory show an average 28-day compressive strength of 10,242 psi.

Table 4.1 28-day compressive strength test results, mixture used at Plant A

Cylinder ID	Age, days	Peak Load, lbf	Compressive Strength, psi
# 1	28	131,900	10,496
# 2	28	124,700	9,923
# 3	28	129,500	10,305
		28-day Average:	**10,242**

4.1.2 Instrumentation

4.1.2.1 Data Acquisition

In Plant A each panel was instrumented using a Campbell Scientific CR5000 data-logger as shown in Figure 4.4. During the fabrication of the panels, each data-logger

was housed inside a waterproof metal enclosure which was then placed inside a wooden box painted orange to increase visibility and protect the electronics. After the panels were transported to and stored at Ferguson Laboratory, all gauges were disconnected from the CR5000, and were connected to single Campbell Scientific CR21 data-logger using Campbell Scientific AM416 Relay Multiplexers. Because each multiplexer could collect 16 channels, two multiplexers were used to multiplex signals from 32 embedment gages in four panels to a single data-logger.

Figure 4.4 Campbell Scientific CR5000 data-logger

4.1.2.2 Strain Gauges

Each panel was instrumented with two different types of strain gages at Plant A. The embedment gages, shown in Figure 4.5, were PMFL-60-8LT manufactured by the Tokyo Sokki Kenkyujo Company. The vibrating wire gages (VWG), shown in Figure 4.6, are Model 4200 manufactured by Geokon, Inc. Eight embedment gages and two vibrating-wire gages were installed in the field at the locations shown in Figure 4.7 and Figure 4.8. As shown in the figures, the gage layout is same for all panels. Gages 4 and 6 are vibrating-wire gages and all others are embedment gages.

Figure 4.5 Embedment gages (Tokyo Sokki Kenkyujo Company)

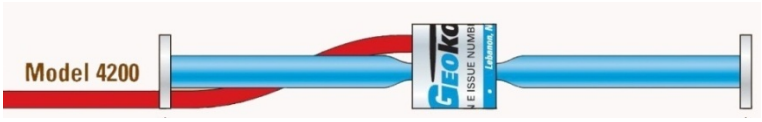

Figure 4.6 Vibrating Wire Gage (Geokon)

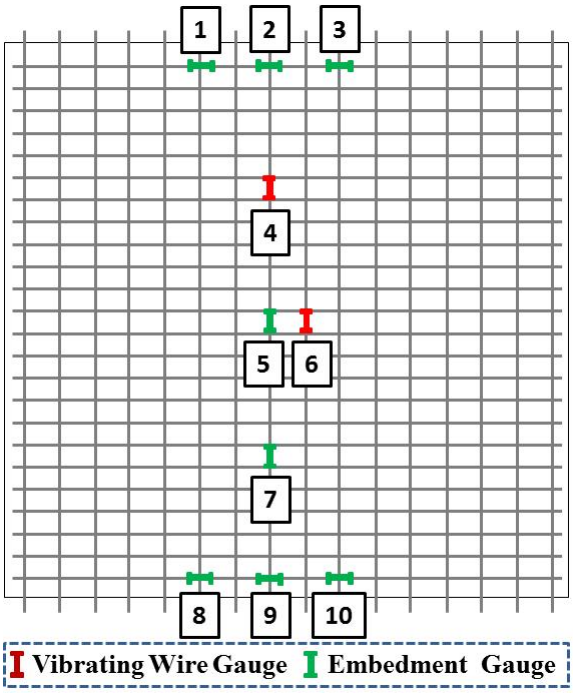

Figure 4.7 Strain-gage layout for Panels C6 and C7

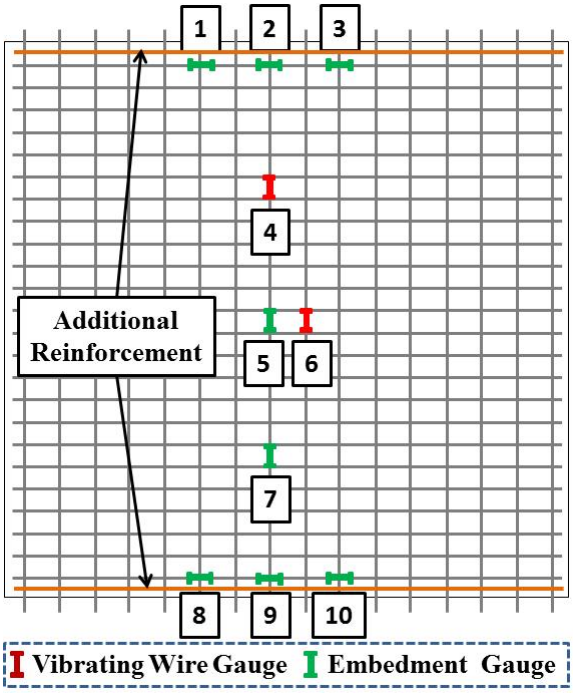

Figure 4.8 Strain-gage layout for Panels M5 and M6

Gages 5 and 7 were installed to collect strain data along the length the panels, which was used to calculate and monitor prestress loss of the strands. The purpose of Gages 1, 2, 3 and 8, 9, 10 is to monitor strain levels at the edge of the panel and help evaluate the effectiveness of additional reinforcement. The purpose of Gages 4 and 6 is to compare readings from the vibrating-wire gages with readings from the embedment gages, and thereby ensure accurate and consistent readings.

The embedment gages and VWGs were installed beneath the reinforcement as shown in Figure 4.9 and Figure 4.10, respectively. The gages were separated by Styrofoam® blocks and were zip-tied securely to the reinforcement. As shown in the figures, the gages were tied at two locations with adequate space in between in order to minimize twisting and to keep the gages parallel to the reinforcing bars. The lead wires were gently tied and routed to the data acquisition system.

Figure 4.9 Embedment gage installed parallel to a prestressing strand (Foreman 2010)

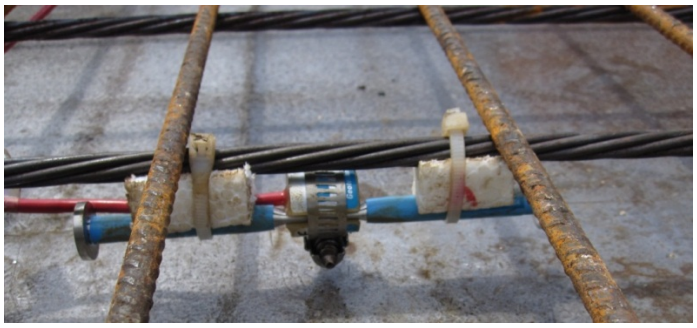

Figure 4.10 Vibrating-Wire Gage installed parallel to a prestressing strand

4.1.3 Fabrication

Installing additional reinforcement and gages on all panels and routing the wires, as shown in Figure 4.11 and Figure 4.12, took approximately two hours.

Figure 4.11 Installing gages at Plant A

Figure 4.12 Gages installed and wires routed, Plant A

Once the researchers finished instrumenting the panels, personnel at Plant A began casting the concrete. As shown in Figure 4.13, the concrete was placed from a "sidewinder" concrete transporter.

Figure 4.13 Casting concrete at Plant A

After shoveling and placing concrete into forms and over the gages, the two-man crew ran the vibrating screed as shown in Figure 4.14. It was expected that the gages should not have been damaged due to dragging the vibrating screed because they were installed beneath the reinforcing bars.

Figure 4.14 Vibrating and screeding concrete at Plant A

Once all concrete placement work was finished, the concrete panels were ponded with water for curing purposes as shown in Figure 4.15.

Figure 4.15 Panels being ponded with water at Plant A

Two days after casting concrete, the researchers returned to Plant A to observe strand release. Before the strands were released, the electronics were checked for proper functioning. To capture elastic shorting at strand release, the strain recording interval was set to 30 seconds. As shown in Figure 4.16, the strands were slowly released by torch-cutting, alternating from one side to the other of the prestressing bed.

Figure 4.16 End strands being torch-cut at Plant A

After the strands at the ends of prestressing bed were released, the strands connecting adjacent panels were cut with a chop saw as shown in Figure 4.17.

Figure 4.17 Interior strands being cut with chop saw at Plant A

After all strands were released, the panels were lifted out of the prestressing bed and stacked three-high as shown in Figure 4.18. The stacked panels were then transported to Plant A's storage area as shown in Figure 4.19. The orange boxes, where the data acquisition was housed, were placed on top of the panels and strapped to the stack.

Figure 4.18 Panels being lifted out of prestressing bed and stacked at Plant A

Figure 4.19 Stacked panels stored at Plant A

4.2 TRANSPORTATION AND STORAGE

Between one and two weeks after casting, the panels were transported to Ferguson Laboratory. The researchers returned to Plant A to confirm that the data acquisition was working properly, and to observe the loading and transportation of the panels. The panels were loaded onto a flatbed truck and were securely strapped using steel chains as shown in Figure 4.20. The straps were aligned with wooden dunnage placed to reduce bending stresses. After delivery to Ferguson Laboratory, the panels were stacked four-high as shown in Figure 4.21. Inspection of the panels showed no cracking after transportation and storage.

Figure 4.20 Panels strapped to flatbed truck, Plant A

Figure 4.21 Panels from Plant A being stacked at Ferguson Laboratory

4.3 PANEL MONITORING

After panels were delivered to Ferguson Laboratory, all instrumented panels were disconnected from the CR5000 and were connected to a single Campbell Scientific CR21 data-logger using multiplexers for long-term monitoring. The CR21 was programmed to

record strain readings every thirty minutes. After one year of monitoring the panels, the strain reading interval was changed to four hours. Data from the data-logger were periodically downloaded and compiled in a master file.

CHAPTER 5
Fabrication and Panel Monitoring at Plant B

5.1 FIELD FABRICATION

Four panels were instrumented and cast at Plant B on September 21st, 2010. The panels were fabricated with a reduced initial prestress of 169.4 ksi, less than the current TxDOT requirement of 189.4 ksi. Two of the four panels were provided with additional transverse reinforcement at each end, and are referred to here as Specimens M7 and M8. The other two panels conformed to current TxDOT requirements, and are referred as Specimens C8 and C9.

5.1.1 Panel Design

Panel design criteria are presented in Section 4.1.1. Sections 5.1.1.1 and 5.1.1.2 discuss the panel reinforcement details and concrete mixture design used by Plant B, as well as the additional reinforcement added by researchers for this project.

5.1.1.1 Reinforcement

As shown in Figure 5.1, Plant B uses D7.5 welded wire mesh at 4-in. spacing for transverse reinforcement and ½ in. diameter prestressing strands at 6-in. spacing for longitudinal reinforcement. The mesh is located below the prestressing strands, and is tied at a few locations after the strands are fully stressed.

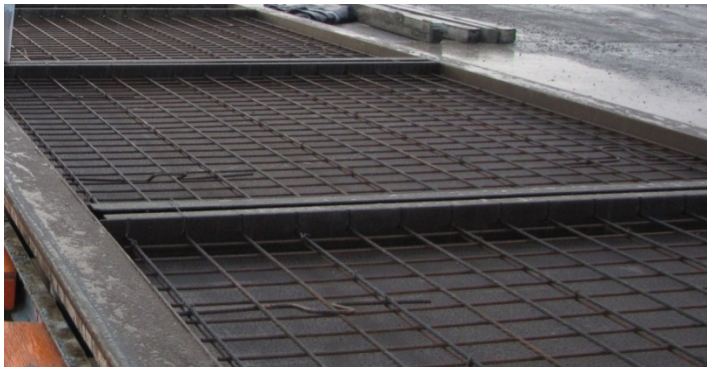

Figure 5.1 Welded wire mesh and strands in place at Plant B

Specimens M7 and M8 were provided with additional transverse reinforcing bars placed 1 in. from each end of the panels. As shown in Figure 5.2, one end of the panel has two additional No. 3 bars stacked vertically and separated by prestressing strands. The other end has additional reinforcement because the welded-wire mesh was placed closer to the end as shown in Figure 5.3.

Figure 5.2 Two additional reinforcing bars at one edge at Plant B

Figure 5.3 One additional reinforcing bar at one edge at Plant B

5.1.1.2 Concrete Mixture Design

Plant B uses river-gravel aggregate for the concrete mixture. Tests performed at Ferguson Laboratory, summarized in Table 5.1, show an average 28-day compressive strength of 8,812 psi.

Table 5.1 28-day compressive strength test results, mixture used at Plant B

Cylinder ID	Age, days	Peak Load, lbf	Compressive Strength, psi
# 1	28	111,300	8,857
# 2	28	106,100	8,443
# 3	28	114,800	9,135
		28-day Average:	**8,812**

5.1.2 Instrumentation

5.1.2.1 Data Acquisition

The same data-acquisition system was used at Plant B as at Plant A. The data-acquisition instrumentation is described in Section 4.1.2.1.

5.1.2.2 Strain Gauges

The instrumentation of each panel at Plant B was similar to that used at Plant A. Each panel was instrumented with two different types of strain gages, whose types and purposes are discussed in in detail in Section 4.1.2.2. Eight embedment gages and two vibrating-wire gages (VWG) were installed in the field at the locations shown Figure 5.4 and Figure 5.5. As shown in those figures, the gage layout is same for all panels. Gages 4 and 6 are vibrating-wire gages, and all others are embedment gages.

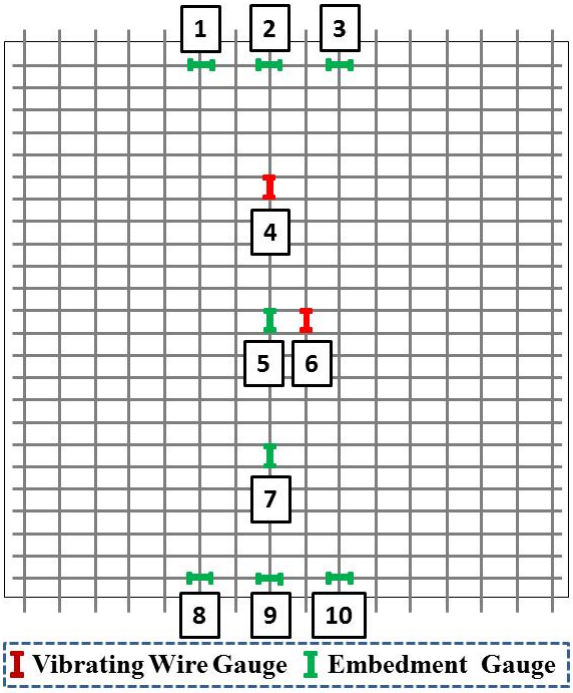

Figure 5.4 Strain-gage layout for Panels C8 and C9

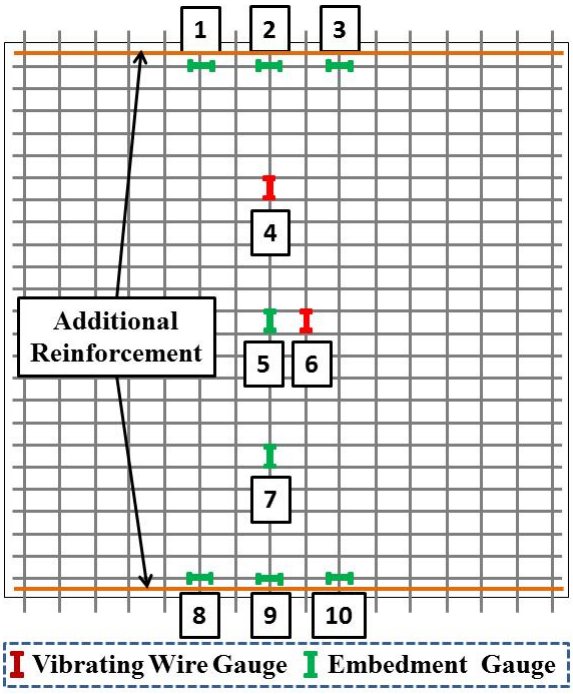

Figure 5.5 Strain-gage layout for Panels M7 and M8

The embedment gages and VWGs were installed beneath the reinforcement as shown in Figure 5.6 and Figure 5.7, respectively. The procedure was similar to that used in Plant A to secure the gages to the reinforcement and route the lead wires.

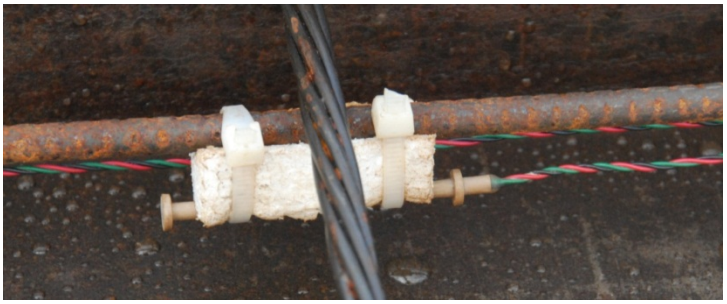

Figure 5.6 Embedment gage installed parallel to a transverse rebar

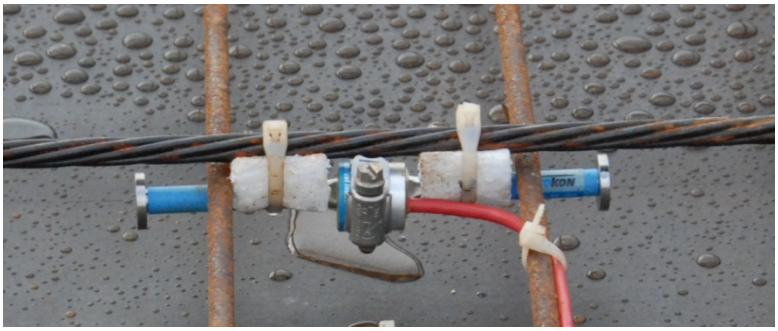

Figure 5.7 Vibrating-Wire Gage installed parallel to a prestressing strand

5.1.3 Fabrication

Installing additional reinforcement, gages on all panels and routing the wires, as shown in Figure 5.8 and Figure 5.9, took approximately two hours.

Figure 5.8 Routing wires at Plant B

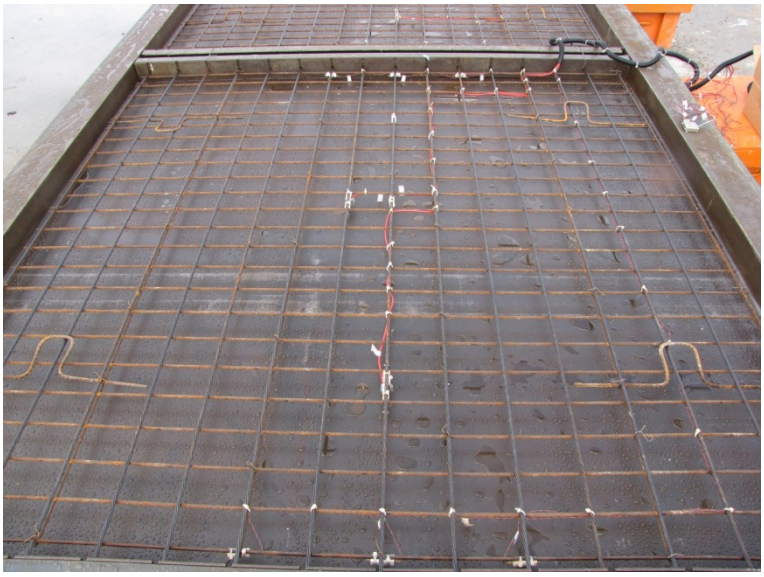

Figure 5.9 Gages installed and wires routed at Plant B

Once the researchers finished instrumenting the panels, personnel at Plant B began casting the concrete. The concrete was placed using a “sidewinder” concrete transporter (Figure 5.10).

Figure 5.10 Casting concrete at Plant B

After shoveling and placing concrete into forms and over the gages, the forms were vibrated and the top surface was finished as shown in Figure 5.11. The vibrating screed could not be lifted over the boxes without disconnecting wires. Before field instrumentation, all lead wires were plugged into a connection box which could be easily connected and disconnected from the data acquisition box. The lead wires were placed in plastic bag to protect against water during the vibration and screeding. It was expected that the gages should not have been damaged due to the moving vibrating screed as the gages were installed beneath the reinforcing bars.

Figure 5.11 Vibrating, screeding and finishing concrete at Plant B

Once all concrete placement work was finished, the concrete panels were covered with wet blankets for curing purposes as shown in Figure 5.12.

Figure 5.12 Panels being covered with wet blankets at Plant B

The day after casting concrete, the researchers returned to Plant B to observe strand release. Before the strands were released all electronics were checked for proper functioning. In order to capture the elastic shorting at strand release, the strain recording interval was set to 30 seconds. As shown in Figure 5.13, the strands were slowly released by torch-cutting, alternating from one side to the other of the prestressing bed.

Figure 5.13 Stands being torch-released at Plant B

After all strands were released, the panels were lifted out of the prestressing bed, stacked and stored three high by the prestressing bed as shown in Figure 5.14. The orange boxes, where the data acquisition was housed, were placed on top of the panels and were strapped to the stack.

Figure 5.14 Panels stacked and stored at Plant B

5.2 TRANSPORTATION AND STORAGE

Two weeks after casting, the panels were transported to Ferguson Laboratory. The researchers returned to Plant B to confirm that the data acquisition was functioning properly, and to observe the loading and transportation of the panels. The panels were loaded onto a flatbed truck and were securely strapped using steel chain links as shown in Figure 5.15. The straps were aligned with dunnage placed to reduce bending stresses. After delivery to Ferguson Laboratory, the instrumented panels were stacked together four-high next to the panels cast in Plant A. Inspection of the panels showed no cracking after transportation and storage.

Figure 5.15 Panels strapped to flatbed truck, Plant B

5.3 PANEL MONITORING

After panels were delivered to Ferguson Laboratory, all instrumented panels were disconnected from CR5000 and were connected to a single Campbell Scientific CR21 data-logger using multiplexers for long term monitoring. The CR21 was programmed to record strain readings every thirty minutes. After one year of monitoring the panels, the strain reading interval was changed to four hours. The data from the data-logger were periodically downloaded and compiled in a master file.

CHAPTER 6

Test Results

In this chapter, observed short-term and long-term prestress losses from "winter" and "summer" panels are compared with predicted values. A total of 14 panels were monitored. The "winter" panels were fabricated in February, 2009 and 2010, using an initial prestress force of 16.1 kips per strand; the "summer" panels were fabricated July, 2010 and September, 2010, using a lower initial prestress force of 14.4 kips per strand. Transverse tensile stresses in panels at release are also reported here.

6.1 PRESTRESS LOSSES

6.1.1 Short-Term Prestress Losses (Elastic Shortening)

6.1.1.1 Estimated elastic losses using 2008 AASHTO Equation

Prestress losses in precast panels due to elastic shortening are estimated using the equation presented in the 2008 AASHTO *LRFD Design Manual* (AASHTO LRFD, 2008) for a prestressed member:

$$\Delta f_{pES} = \frac{A_{ps} f_{pbt} \left(I_g + e_m{}^2 A_g\right) - e_m M_g A_g}{A_{ps}\left(I_g + e_m{}^2 A_g\right) + \frac{A_g I_g E_{ci}}{E_p}} \qquad \text{(Equation C5.9.5.2.3a-1)}$$

When this equation is applied to a PCP panel with the current TxDOT-specified initial prestress of 16.1 kips per strand, the specified compressive strength of 4,000 psi, the corresponding elastic modulus of 3,740 ksi, and an assumed concrete unit weight of 147.5 lb/ft^3, prestress losses due to elastic shortening are 5.1 ksi. For a PCP panel with a lower initial prestress of 14.4 kips per strand, prestress losses due to elastic shortening are 4.5 ksi. Predicted and measured values are compared in Table 6.1.

6.1.1.2 Measured elastic losses

Strain readings in panels were recorded at 30-second intervals during strand release. These strains were then used to monitor stress levels in the prestressing strands. The largest prestress loss occurred in the center of the panel where strains were measured by Gage #5 (gage locations as shown in Figure 4.7 and Figure 4.8). Figure 6.1 and Figure 6.2 show the stress changes in panels cast at Plants A and B, respectively. Release data for Specimen C6 from Plant A were lost due to malfunction of the data-acquisition system.

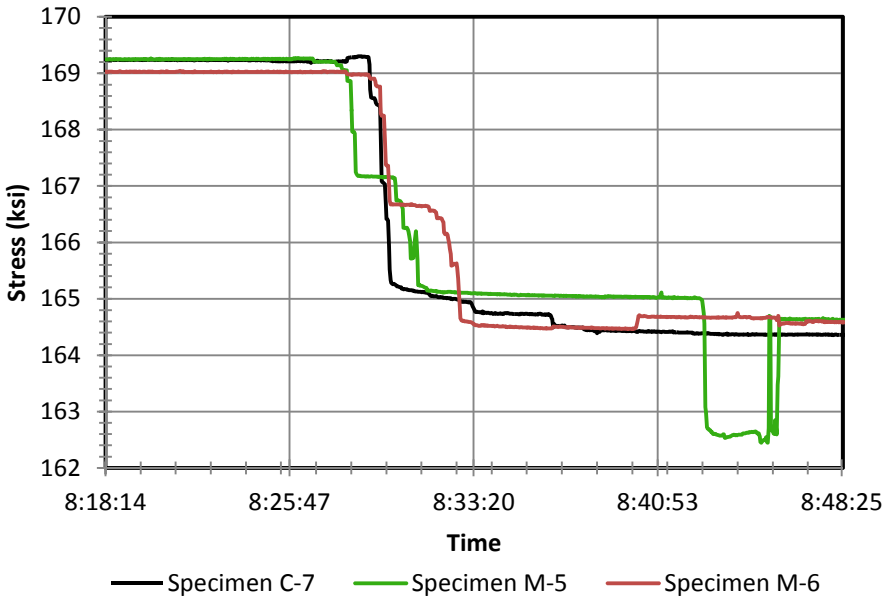

Figure 6.1 Stresses in prestressing strands in "summer" panels during release, Plant A

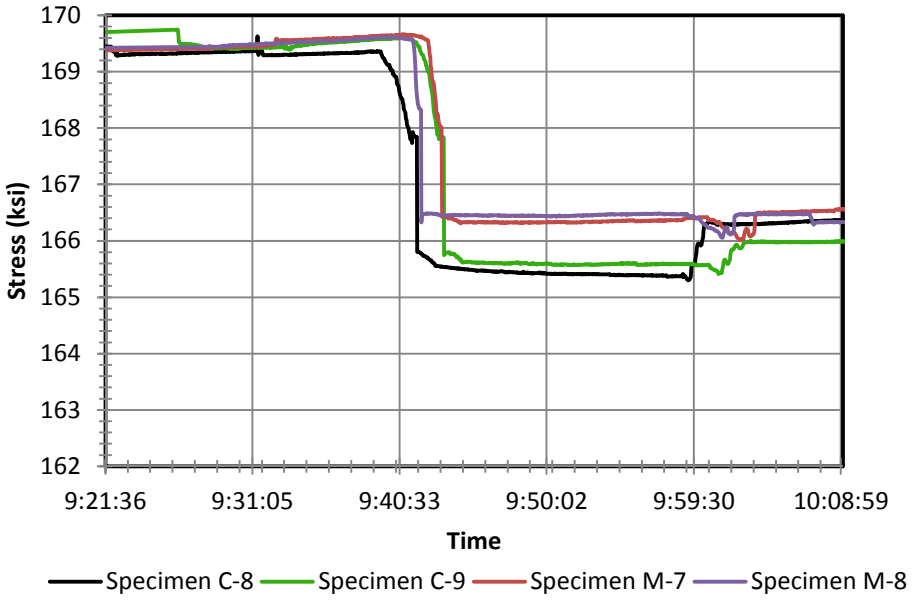

Figure 6.2 Stresses in prestressing strands in "summer" panels during release, Plant B

As shown in Figure 6.1 and Figure 6.2, the average prestress losses due to elastic shortening in Plant A and Plant B panels were 4.4 ksi and 3.6 ksi, respectively. In addition to embedment gages, vibrating wire gages (VWG) were installed near Gage #5 in all panels. According to strains recorded by VWG before and after release of strands, the average prestress losses in Plant A and Plant B panels were 4.3 ksi and 3.1 ksi, respectively. Measured values of elastic shortening in each panels at two different plants and at different seasons are summarized in Table 6.1 along with the predicted values calculated using the 2008 AASHTO.

Table 6.1 Calculated versus measured prestress losses due to elastic shortening (ksi)

Winter Panels			**Summer Panels**		
AASHTO 2008			AASHTO 2008		
Eq. (5.9.5.2.3a-1)	**5.0**		Eq. (5.9.5.2.3a-1)	**4.5**	
Plant A Panels	Gage #6		Plant A Panels	Gage #5	VWG
C2	4.0		C7	4.2	4.1
M1	3.3		M5	4.2	4.7
M2	3.1		M6	4.7	4.2
Average	**3.5**		***Average***	**4.4**	**4.3**
Plant B Panels	Gages #10	VWG	Plant B Panels	Gage #5	VWG
C4	3.0	3.2	C8	3.9	3.1
C5	3.1	3.1	C9	4.0	3.4
M3	3.1	3.1	M7	3.3	3.1
M4	3.4	2.9	M8	3.2	2.8
Average	**3.2**	**3.1**	***Average***	**3.6**	**3.1**

6.1.2 Long-Term Prestress Losses (Creep, Shrinkage, and Relaxation)

6.1.3 Estimated Long-term Losses

Design of precast prestressed panels is highly standardized by TxDOT, and the design is intended to follow AASHTO *Bridge Design Specifications* (Merrill, 2002). In 2009 and 2010 (when panels were fabricated), TxDOT designed bridges to meet the 2004 AASHTO *Specifications*. The 2004 AASHTO equations predict total prestress loss of 24.2 ksi for both "winter" and "summer" panels. However, the 2008 AASHTO *Specification* incorporated major changes, including using refined time-dependent variables in predicting long-term prestress losses. The ultimate prestress losses calculated

at 10,000 days using the 2008 AASHTO equations result in predicted long-term losses of 34.0 ksi and 31.2 ksi for “winter” and “summer” panels, respectively. Predicted losses for individual panels at their respective ages during analysis are presented in Table 6.2 and Table 6.3. Calculations based on 2004 and 2008 AASHTO equations are provided in the Appendix.

6.1.4 Observed Long-term Losses

After strand release, the strain-recording interval was set to 30 minutes in each panel. About five months after casting, strand stresses began to stabilize. About one year after casting, the strain-recording interval was set to four hours. Six “winter” panels and eight “summer” panels have been continuously monitored since casting to provide accurate value of prestress losses in PCPs.

Plant A uses crushed limestone coarse aggregates and Plant B uses river gravel coarse aggregates. To better understand the effects of daily temperature variations on concrete long-term properties, the coefficient of thermal expansion (CTE) was assumed to be constant, with values of 6×10^{-6} /°C for river-gravel aggregates and 7.5×10^{-6} /°C for limestone aggregates (Foreman, 2010; Emanuel *et al.*, 1987).

Because the highest prestress losses were expected to occur in the center of the panels, each panel had an embedment gage parallel to a middle strand at the panel center. Except for the “winter” panels cast at Plant A, all panels had additional VWG near the center of the panel as an independent check on the embedment gages.

6.1.4.1 Long-term Losses in “Winter” Panels

Figure 6.3, Figure 6.4, Figure 6.5, Figure 6.6, Figure 6.7, and Figure 6.8 show long-term strand stresses in current and modified “winter” panels fabricated at Plants A and B. Stresses in panels from Plant A and Plant B are calculated from strain readings obtained from Gage #6 and Gage #10 (center gages), respectively. The layout of gages in “winter” panels is given in Foreman (2010).

The strands in "winter" panels were initially stressed to 189.4 ksi, corresponding to the TxDOT-specified initial prestress of 16.1 kips per strand.

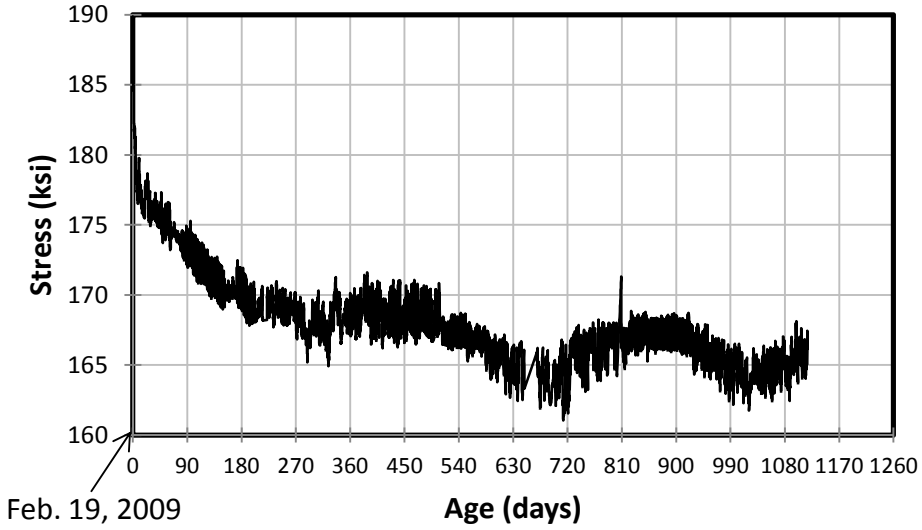

Figure 6.3 Long-term stresses in "winter" Panel C2 cast at Plant A

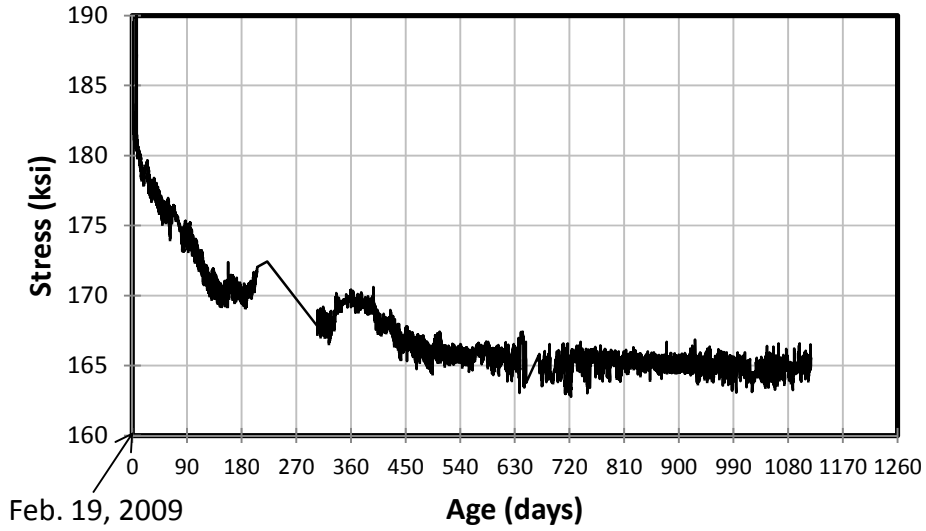

Figure 6.4 Long-term stresses in "winter" Panel M2 cast at Plant A

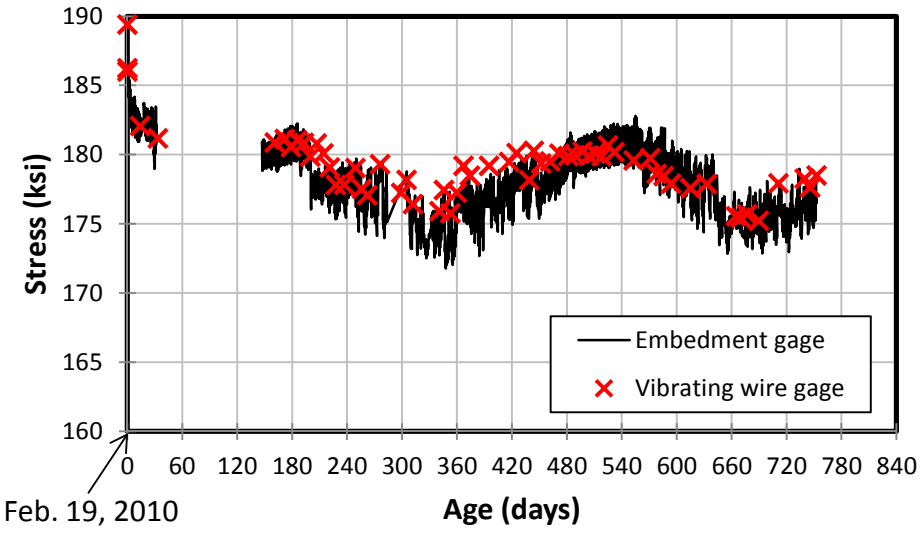

Figure 6.5 Long-term stresses in "winter" Panel C4 cast at Plant B

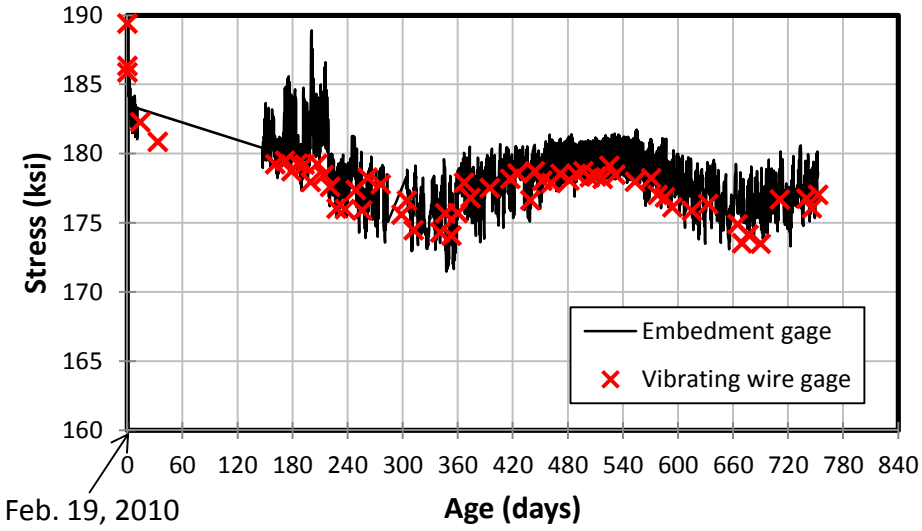

Figure 6.6 Long-term stresses in "winter" Panel C5 cast at Plant B

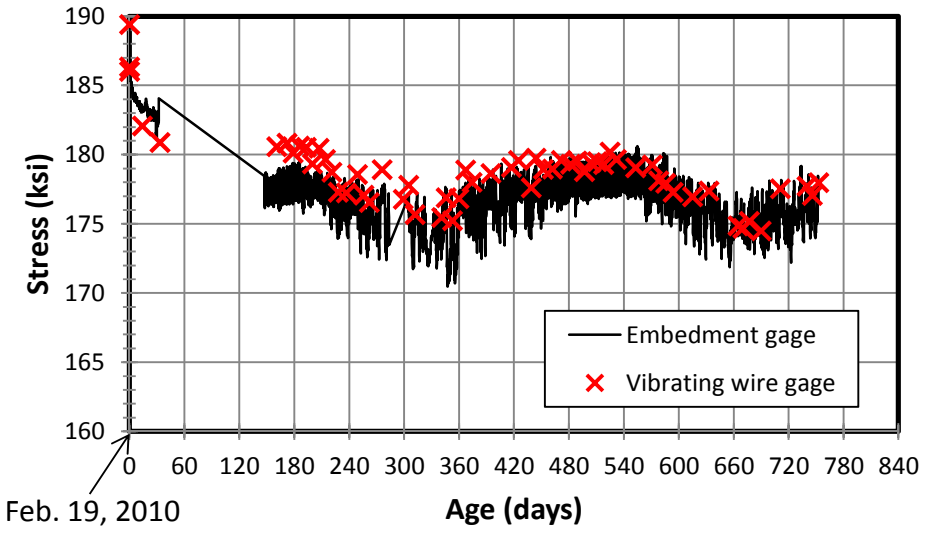

Figure 6.7 Long-term stresses in "winter" Panel M3 cast at Plant B

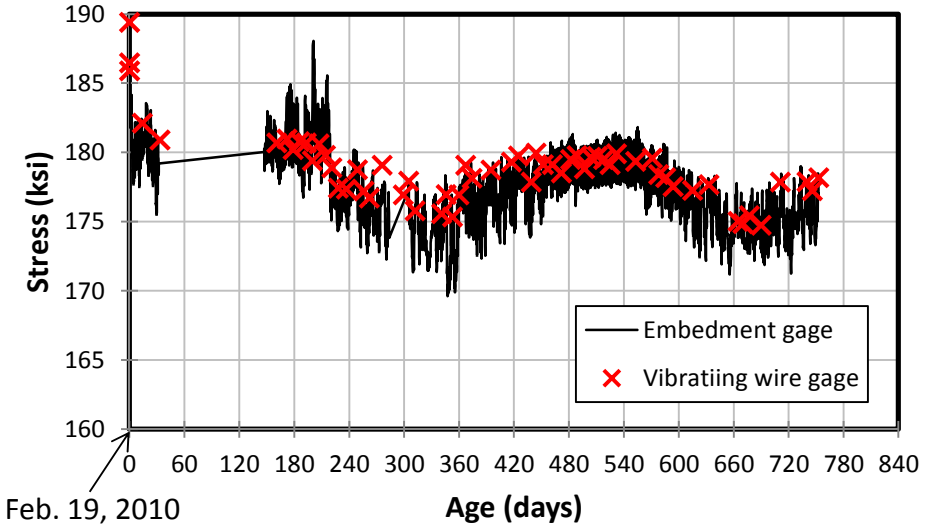

Figure 6.8 Long-term stresses in "winter" Panel M4 cast at Plant B

Long-term results from "winter" panels show that the highest prestress losses (24.4 ksi in Panels C2 and M2) occurred in panels cast at Plant A, at an age of about 37 months. These losses are 5% higher than those observed by Foreman (2010) at an age of about 13 months. The average of observed prestress losses in Plant B panels was 12.4 ksi. Figure 6.9 shows long-term strand stresses in all "winter" panels, along with the

effective prestress levels predicted using 2004 AASHTO equations, 2008 AASHTO equations, and current TxDOT practice.

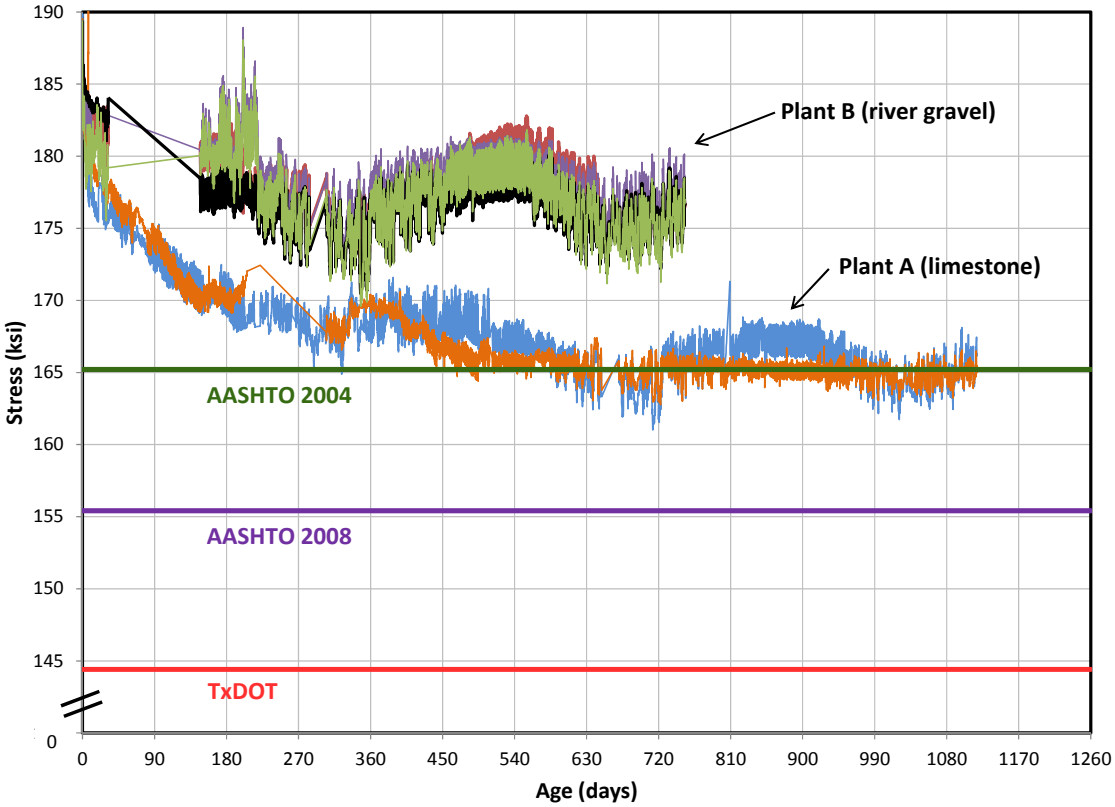

Figure 6.9 Long-term stresses in "winter" panels (embedment gages)

Table 6.2 presents the numeric values of prestress losses in "winter" panels directly estimated from Figure 6.9, VWGs and using the code equations. The prestress-loss equations of 2008 AASHTO allow estimating losses at a given age. When these equations are applied at the date when the data are analyzed, the total prestress losses are 33.0 ksi and 32.6 ksi for Plant A and Plant B panels, respectively. Also, 2004 and 2008 AASHTO predicted ultimate prestress losses at 10,000 days are presented in Table 6.2. As shown in the table, the 2008 AASHTO method predicted greater prestress losses, 28% and 64% for Plant A and Plant B panels, respectively. The 2004 AASHTO method predicted the losses most accurately.

Assuming the prestress losses have stabilized in Plant B panels, it can be concluded from Figure 6.9 and Table 6.2 that the average long-term losses are 50% higher for the limestone aggregate panels than the river-gravel aggregate panels.

Table 6.2 Summary of long-term prestress losses and predictions for "winter" panels

Plant A Panels	Age (days)	Embedment gage (ksi)	VWG (ksi)	AASHTO 2008 (ksi)
C2	1118	24.4	-	33.0
M2	1118	24.4	-	33.0
Average		**24.4**		**33.0**
Plant B Panels				
C4	753	12.1	10.9	32.6
C5	753	11.7	12.5	32.6
M3	753	13.1	11.6	32.6
M4	753	12.9	11.4	32.6
Average		**12.4**	**11.6**	**32.6**
	AASHTO 2004	AASHTO 2008		
At 10,000 days	24.2	34.0		

6.1.4.2 Long-term Losses in "Summer" Panels

Figure 6.10, Figure 6.11, Figure 6.12, and Figure 6.13 show long-term strands stresses in current and modified "summer" panels fabricated at Plant A. Figure 6.14, Figure 6.15, Figure 6.16, and Figure 6.17 show long-term strand stresses in current and modified "summer" panels fabricated at Plant B. Stresses in these panels were calculated from strain readings obtained from center Gage #5 (gage locations as shown in Figure 4.7 and Figure 4.8). The strands in "summer" panels were initially stressed to 169.4 ksi, corresponding to a lower initial prestress of 14.4 kips per strand.

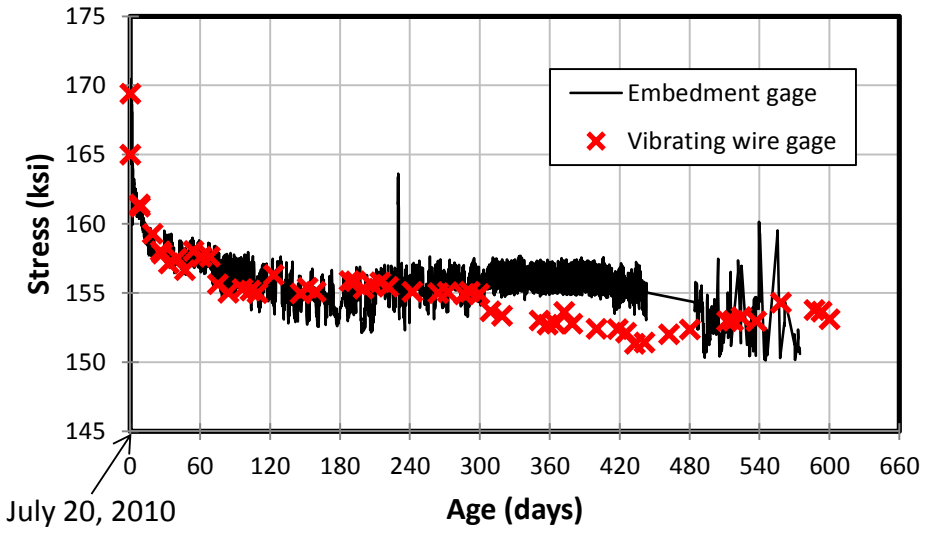

Figure 6.10 Long-term stresses in "summer" Panel C6 cast at Plant A

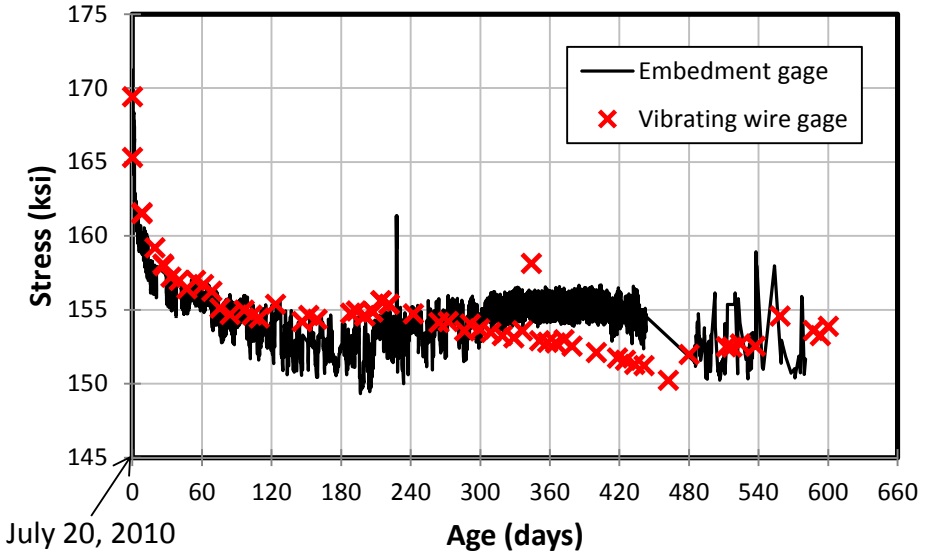

Figure 6.11 Long-term stresses in "summer" Panel C7 cast at Plant A

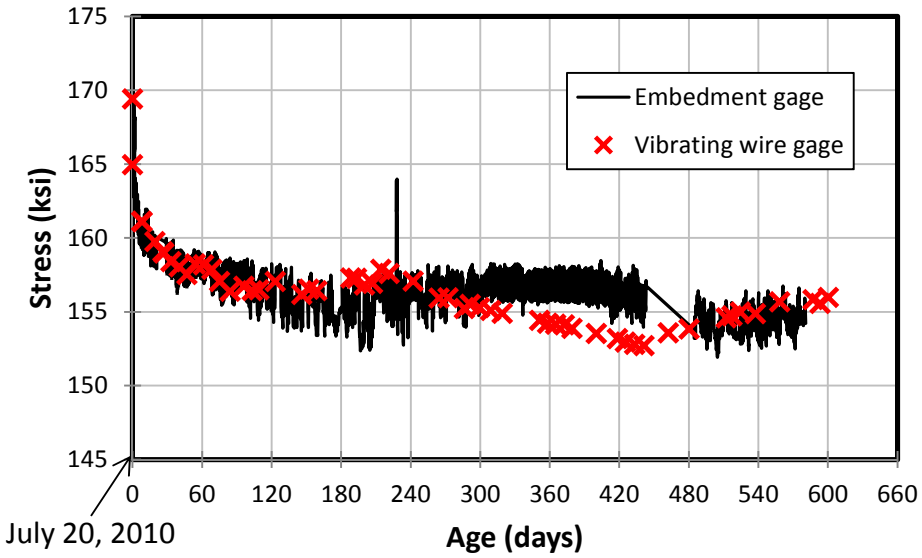

Figure 6.12 Long-term stresses in "summer" Panel M5 cast at Plant A

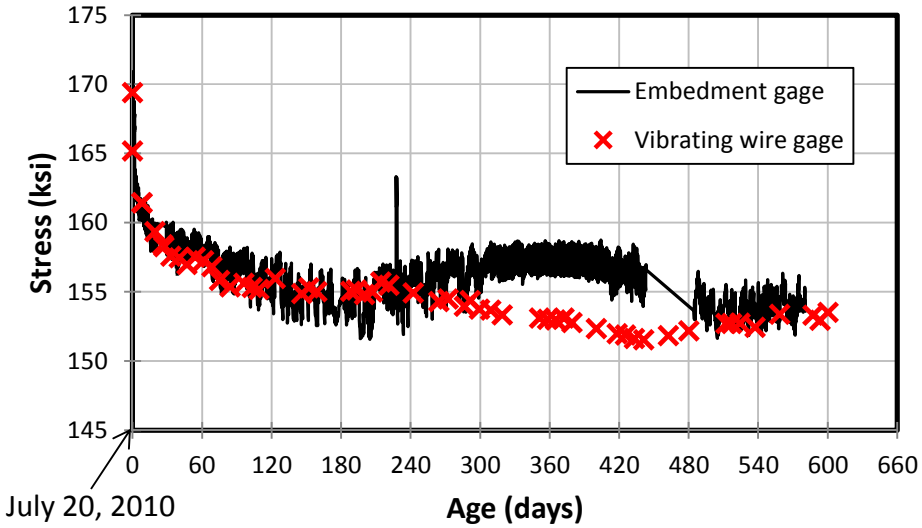

Figure 6.13 Long-term stresses in "summer" Panel M6 cast at Plant A

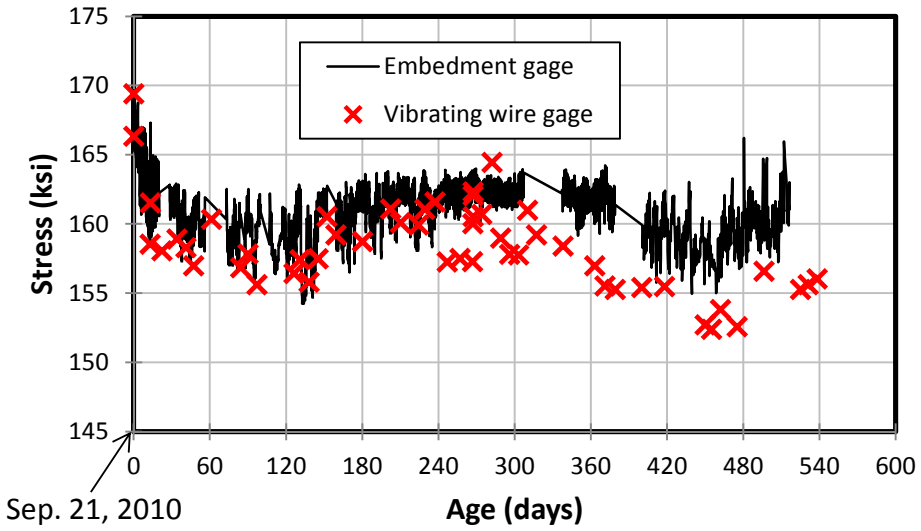

Figure 6.14 Long-term stresses in "summer" Panel C8 cast at Plant B

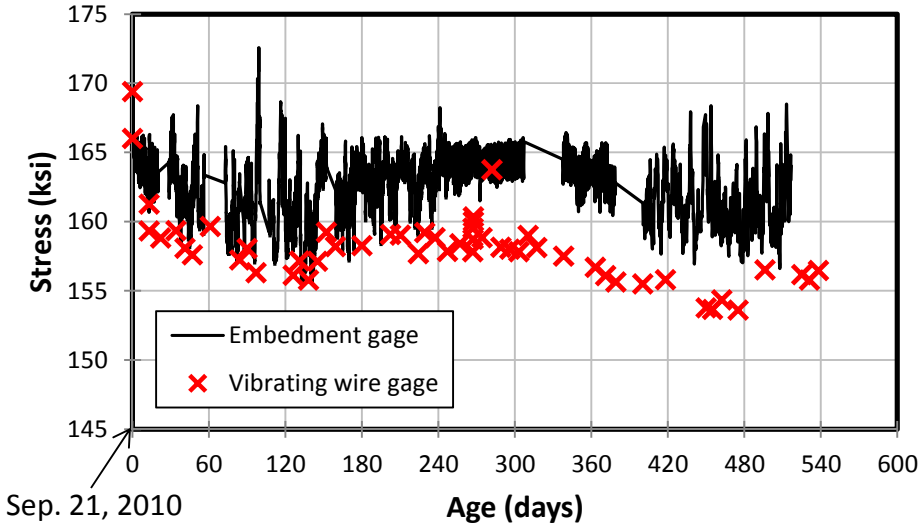

Figure 6.15 Long-term stresses in "summer" Panel C9 cast at Plant B

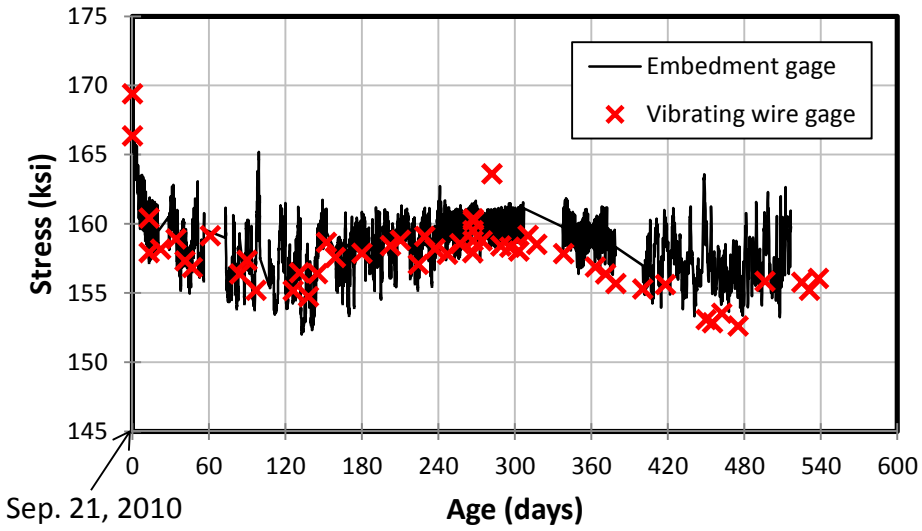

Figure 6.16 Long-term stresses in "summer" Panel M7 cast at Plant B

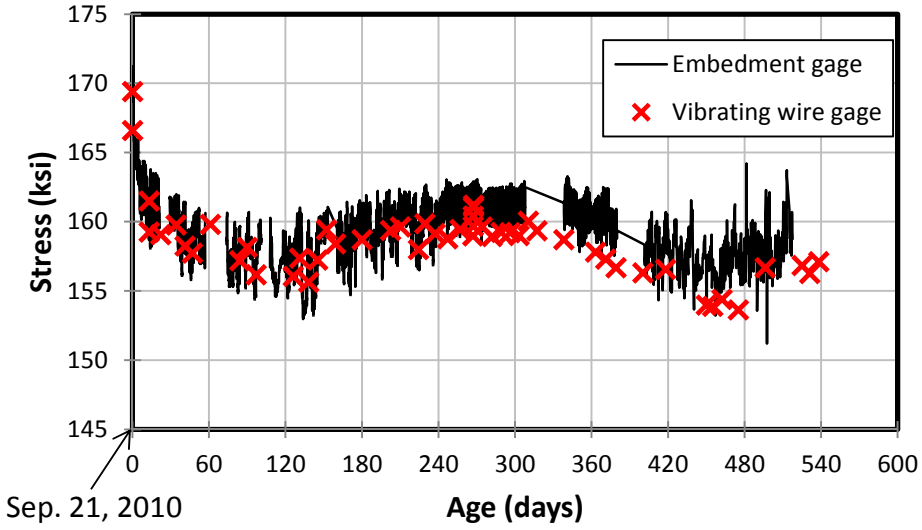

Figure 6.17 Long-term stresses in "summer" Panel M8 cast at Plant B

Long-term results from "summer" panels show that the highest prestress losses (15.6 ksi in Panel C7) occurred in panels fabricated at Plant A, at an age of more than 17 months. The average of observed prestress losses in Plant B panels was 11.1 ksi. Figure 6.18 shows long-term strand stresses in all "summer" panels along with the effective

prestress levels predicted using 2004 AASHTO equations, 2008 AASHTO equations, and current TxDOT practice.

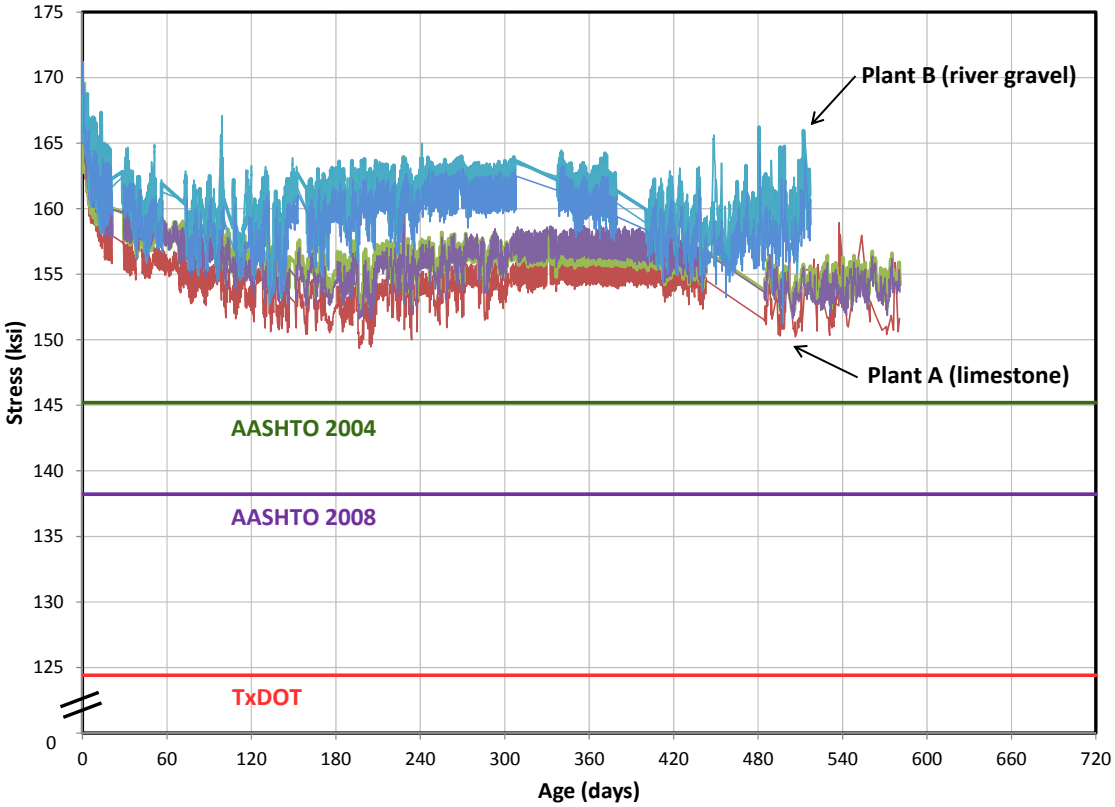

Figure 6.18 Long-term stresses in "summer" panels (embedment gages)

Table 6.3 presents the numeric values of prestress losses in "summer" panels directly estimated from Figure 6.18, VWGs and using the code equations. When 2008 AASHTO method is used at the date when the data are analyzed, the total prestress losses are 29.4 ksi and 29.3 ksi for Plant A and Plant B panels, respectively. Also, 2004 and 2008 AASHTO predicted ultimate prestress losses at 10,000 days are shown in Table 6.3. As shown in the table, 2008 AASHTO method gave the prestress losses that exceeded measured values by more than 50% on average for Plant A and Plant B panels. The 2004 AASHTO method also gave losses about 50% greater than measured.

If the prestress losses have stabilized in Plant A and Plant B panels, it can be concluded from Figure 6.18 and Table 6.3 that the average long-term losses are 20%

higher for the limestone aggregate panels than the river-gravel aggregate panels when all the panels are fabricated with the lower initial prestress.

Table 6.3 Summary of long-term prestress losses and predictions for "summer" panels

Plant A Panels	Age (days)	Embedment gage (ksi)	VWG (ksi)	AASHTO 2008 (ksi)
C6	580	14.2	15.6	29.4
C7	580	15.6	15.8	29.4
M5	580	13.8	14.8	29.4
M6	580	13.9	15.9	29.4
Average		**13.8**	**15.3**	**29.4**
Plant B Panels				
C8	520	11.4	11.3	29.3
C9	520	10.4	11.8	29.3
M7	520	11.2	12.0	29.3
M8	520	11.3	11.2	29.3
Average		**11.1**	**11.6**	**29.3**
	AASHTO 2004	AASHTO 2008		
At 10,000 days	24.2	31.2		

6.1.4.3 Summary of "Winter" and "Summer" Panels

Based on long-term monitoring of precast prestressed concrete panels fabricated at two different Texas precast plants and at two different seasons, the following observations and summaries are made:

1) Prestress losses in panels stabilized about five months after casting;

2) Prestress losses are lower for panels fabricated with river-gravel coarse aggregates than limestone coarse aggregates;

3) On average, prestress losses are 10% and 8% of the initial prestress for "winter" and "summer" panels, respectively;

4) The highest observed prestress loss was 24.4 ksi;

5) The 2004 AASHTO method predicts the actual prestress losses more closely than 2008 AASHTO method and current TxDOT practice;

6) TxDOT approach of assuming a 45-ksi lump sum in prestress losses is quite conservative (high);

7) On average, readings obtained from embedment gages and VWGs show good agreement.

6.2 TRANSVERSE TENSILE STRESSES DURING RELEASE

The tensile strength of concrete is highly variable, and several methods are available for predicting it. Three most commonly used methods are $4\sqrt{f'_c}$ (Direct Tension), $6\sqrt{f'_c}$ (Split Cylinder), and $7.5\sqrt{f'_c}$ (Modulus of Rupture) (Tuchscherer, 2009). Using an average of compressive strengths reported by Plants A and B of 6,500 psi at release, the tensile strength of concrete would be 322 psi, 484 psi and 605 psi according to three methods, respectively.

Table 6.4 summarizes the recorded maximum tensile strains and calculated tensile stresses at panel edges during release for the panels cast with a lower initial prestress. The modulus of elasticity was calculated based on the average compressive strength at release. As shown in the table, the maximum calculated tensile stress is 221 psi in Panel C8, which is smaller than the tensile strength predicted by any of the above methods. This is confirmed by the visual observation of no cracks in the field. For comparison purposes, Table 6.5 summarizes the recorded maximum tensile strains and calculated tensile stresses at panel edges during release for the panels cast with a higher initial prestress. As shown in the table, the maximum stress is still smaller than the tensile strength predicted by any of the above methods even with a higher initial prestress.

Table 6.4 Summary of maximum observed tensile strains and calculated tensile stresses at panel edges during release (with lower initial prestress)

Plant	Panel	Strain (in/in)	Tensile Stress (psi)
A	C7	0.000033	151
A	M5	0.000028	128
A	M6	0.000012	55
Average			***111***
B	C8	0.000048	221
B	C9	0.000038	175
B	M7	0.000030	137
B	M8	0.000036	164
Average			***175***

Table 6.5 Summary of maximum observed tensile strains and calculated tensile stresses at panel edges during release (with higher initial prestress) (Foreman 2010)

Plant	Panel	Strain (in/in)	Tensile Stress (psi)
A	C2	0.00004	184
A	M1	0.000023	106
A	M2	0.000028	129
Average			***140***
B	C4	0.00005	230
B	C5	0.000036	165
B	M3	0.000019	87
B	M4	0.00003	138
Average			***207***

CHAPTER 7
Summary, Conclusions, and Recommendations

7.1 SUMMARY OF THESIS

Precast, prestressed concrete panels (PCPs) are widely used by the Texas Department of Transportation (TxDOT) as stay-in-place forms in bridge deck construction. Those panels are required to be designed assuming a 45-ksi lump-sum prestress loss. Some panels have experienced problems with collinear cracks (cracks along the lengths of the strands). One reason for these collinear cracks is believed to be the required level of initial prestress, which might be reduced if experimentally observed prestress losses were shown to be less than the assumed value. For this purpose, 20 precast, prestressed panels were cast at two different plants. Half of those 20 panels were fabricated with the current TxDOT-required prestress of 16.1 kips per strand, and the other half were fabricated with a lower prestress of 14.4 kips per strand based on initially observed prestress losses of 25 ksi or less (Foreman, 2010). Thirteen of those panels were instrumented with strain gages and monitored over their life time. Observed losses stabilized after five months, and are found to be about 24.4 ksi. Even with the reduced initial prestress, the remaining prestress in all panels exceeds the value now assumed by TxDOT for design.

7.2 CONCLUSIONS

The following conclusions were derived from the research project:

1) Formation of longitudinal cracks along the strands can be attributed to many factors. One factor is the applied initial prestress force. When the strands are released, large forces are transferred to the panels. Due to these forces the strands tend to increase in diameter due to the Hoyer effect and, thereby, produce circumferential tensile stresses in the concrete. When the tensile stresses exceed the

tensile strength of concrete, cracks form radially around the strands and propagate longitudinally collinear to the strands.

2) Other factors contributing to collinear cracks include improper handling and transportation, and storage (Foreman, 2010). Undesired levels of stresses could develop if panels, once released, are improperly handled and transported for storage. Panels must be secured carefully to the truck bed to avoid the creation of bending stresses. Adequate support and enough storage area must be provided for the deck panels to avoid damage to the panels both at the plant and job site.

3) Long-term monitoring of thirteen panels show that the average long-term prestress losses are about 10% and 8% of initial prestress for PCPs cast in winter and summer, respectively.

4) Prestress losses are consistently lower for panels fabricated with river-gravel aggregates than for panels fabricated with limestone aggregates.

5) The TxDOT assumption of 45-ksi lump-sum prestress losses is very conservative for the design PCPs.

7.3 RECOMMENDATIONS

1) Long-term monitoring of PCP's cast in winter and summer with current and reduced applied initial prestress force suggests that currently assumed lump-sum prestress loss of 45 ksi can be reduced to 25 ksi.

2) A reduction of initial prestress force from 16.1 kips per strand to 14.4 kips per strand is consistent with estimated prestress loss of 25 ksi. With reduced initial prestress force, cracks would form less often.

3) Although measured strains did not indicate cracking nor were any cracks found in the panels studied, the use of additional transverse reinforcing bars at the edges of panels could help control the width and growth of collinear cracks. These bars can be placed 1 in. from each end of the panels, perpendicular to the strands.

APPENDIX

A.1 TxDOT CAD Standards

TxDOT CAD standards on precast, prestressed concrete panel fabrication placement details are presented in this section.

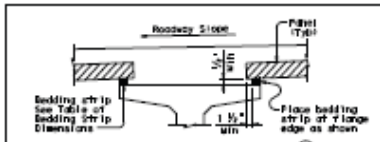

NORMAL GRADING DETAIL ①

Showing Prestressed Concrete I-Girders. (Other Beam Types Similar)

TABLE OF BEDDING STRIP DIMENSIONS		
WIDTH	HEIGHT ②	
	Min	Max
1" (Min)	½"	2"
1 ½"	½"	2 ½"
1 ½"	½"	3"
1 ½"	½"	3 ½"
2" (Max)	½"	4"

① To reduce the quantity of cast-in-place concrete, bedding strip thickness may be increased in ½" increments. Bedding strips must be comprised of one layer. Bond bedding strips to the beams with an adhesive compatible with bedding strips. Bedding strips over 2.5" high may need to be bonded to panels. The same thickness strip must be used under any one panel edge and the maximum change in thickness between adjacent panels is ½". Alternatively, bedding strips may be cut to grade. Panels may be supported by an alternate method, using a commercial product, if approved by the Engineer of Bridge Design, Bridge Division.

② Height must not exceed twice the width.

③ Clear cover shall be as indicated unless otherwise shown on Span Details.

④ See Span Details for top slab reinforcement and clear cover. Longitudinal top slab reinforcement may rest on top of prestressed concrete panels if necessary to maintain clear cover.

⑤ Space Bars UP(#4) with Beam Bars R(#4) in all areas where measured haunch exceeds 3" or 3 ½" with Prestressed Concrete I-Girders. Epoxy coating for Bars UP is not required.

⑥ Construction joints cannot be located on top of a panel.

⑦ Butt adjacent bedding strips together with adhesive. Cut v-notches, approx ¼" deep, in the top of the bedding strips at 8' o.c..

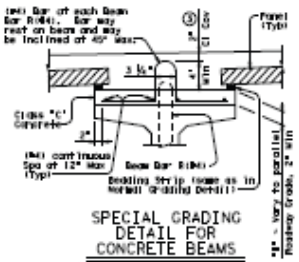

SPECIAL GRADING DETAIL FOR CONCRETE BEAMS

Showing Prestressed Concrete I-Girders. (Other Beam Types Similar)

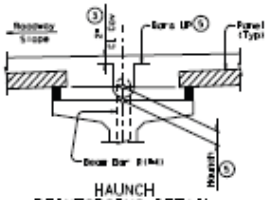

HAUNCH REINFORCING DETAIL

Showing Prestressed Concrete I-Girders. (Other Beam Types Similar)

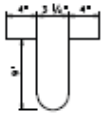

BARS UP (#4) ⑤

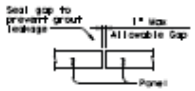

TYPICAL SECTION AT PANEL JOINT

(Panel reinforcing not shown for clarity.) The gap cannot be considered as a panel fabrication tolerance.

CONSTRUCTION NOTES:

Erected panels must bear uniformly on bedding strips of extruded polystyrene placed along top flange edges.

If additional blocking is needed, special grading details for supporting the panels and extra reinforcing between beam and slab will be considered subsidiary to deck construction.

Bars U, shown on PCP-FAB, may be bent over or cut off if necessary.

Care must be taken to ensure proper cleaning of construction debris and consolidation of concrete mortar under the edges of the panels. Bedding strips must be placed on beam flange edges so that adequate space is provided for the mortar to flow a minimum of ½" under the panels as the slab concrete is placed.

To allow the proper amount of mortar to flow between beam and panel, the minimum vertical opening must be at least ½". Roadway cross-slope reduces the opening available for entry of the mortar. Bedding strips varying in thickness across the beam are therefore required.

All reinforcing steel in the cast-in-place slab must be Grade 60. See Table of Reinforcing Steel for size and spacing of reinforcement.

If the top and bottom layer of reinforcing steel is shown on the Span Details to be epoxy coated, then the D, E, F, & Z bars must be epoxy coated.

For clear span between U-beams less than or equal to 18', see Permissible Slab Forming Detail on Miscellaneous Slab Detail sheets, LRMS.

Bar Laps, where required, must be as follows:

Uncoated	- #4 = 1'-5" - #5 = 1'-9" - #6 = 2'-1"
Epoxy Coated	- #4 = 2'-1" - #5 = 2'-7" - #6 = 3'-1"

GENERAL NOTES:

Designed according to AASHTO LRFD Specifications.

Panel placement may follow either Option 1 or Option 2 except Option 1 must be used where the slab is continuous over Inverted-T bents or if the skew exceeds 45 degrees.

Use of Prestressed Concrete Panels is not permitted for non-parallel curved steel girders or tub girders. See Span Details for other possible restrictions on their use.

These details are to be used in conjunction with the Span Details, PCP-FAB and other applicable Standard sheets.

Any additional reinforcement or concrete required on this standard is to be considered subsidiary to the bid item "Reinforced Concrete Slab".

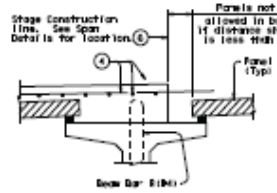

PRESTR CONC I-GIRDERS

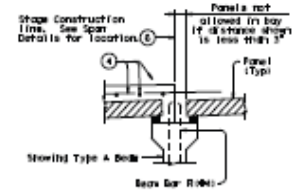

PRESTR CONC I-BEAMS

STAGE CONSTRUCTION LIMITATIONS

(Other Beam Types Similar)

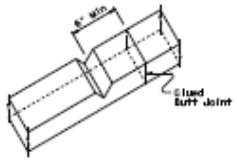

BEDDING STRIP DETAIL ⑦

HL93 LOADING SHEET 1 OF 4

Texas Department of Transportation
Bridge Division

PRESTRESSED CONCRETE PANELS OPTIONAL DECK DETAILS

PCP

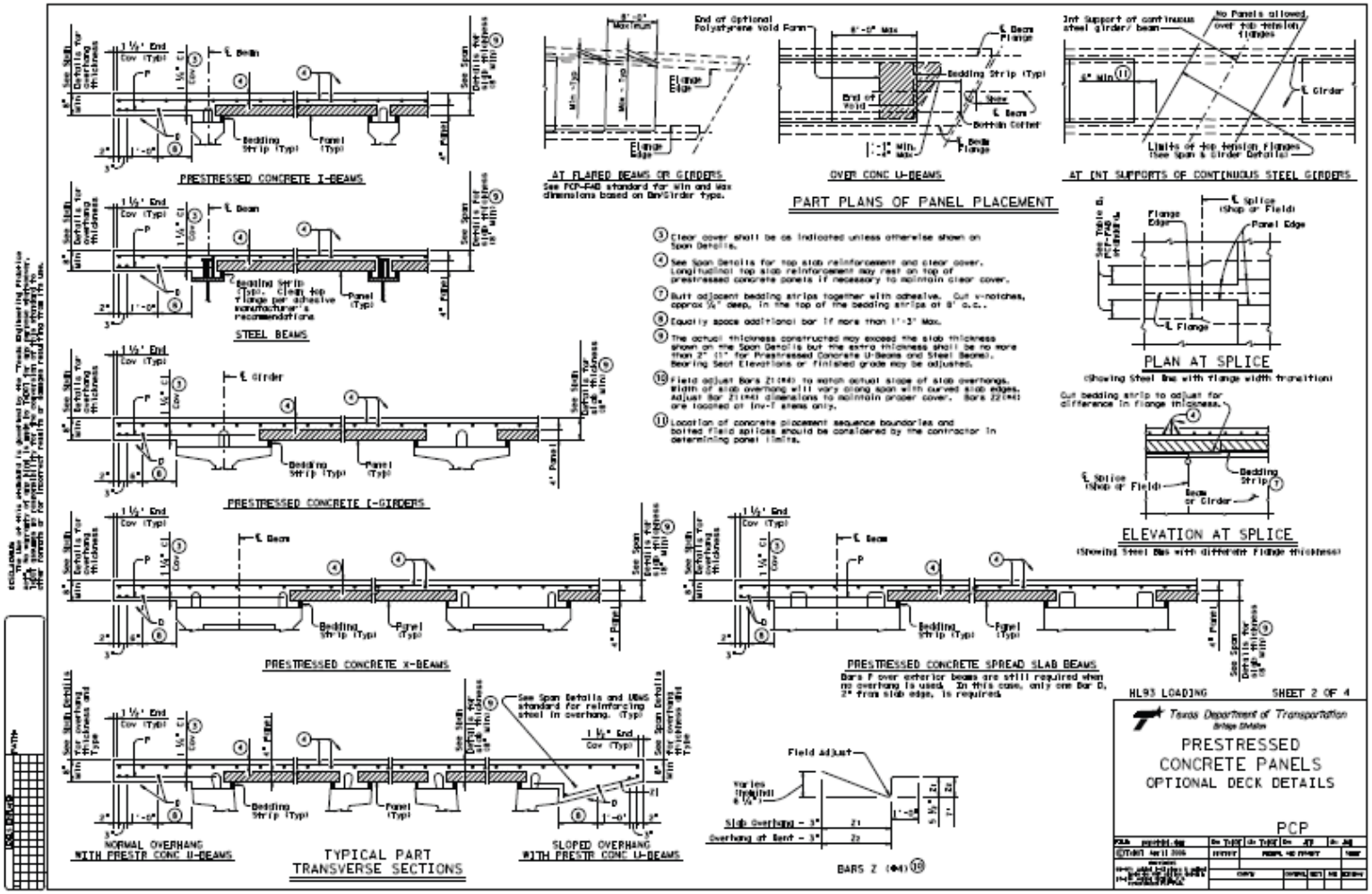
PRESTRESSED CONCRETE I-BEAMS
STEEL BEAMS
PRESTRESSED CONCRETE C-GIRDERS
PRESTRESSED CONCRETE X-BEAMS
NORMAL OVERHANG WITH PRESTR CONC U-BEAMS
SLOPED OVERHANG WITH PRESTR CONC U-BEAMS
TYPICAL PART TRANSVERSE SECTIONS
AT FLARED BEAMS OR GIRDERS
See PCP-FAD standard for Min and Max dimensions based on Bm/Girder type.
OVER CONC U-BEAMS
AT INT SUPPORTS OF CONTINUOUS STEEL GIRDERS
PART PLANS OF PANEL PLACEMENT
3 Clear cover shall be as indicated unless otherwise shown on Span Details.
4 See Span Details for top slab reinforcement and clear cover. Longitudinal top slab reinforcement may rest on top of prestressed concrete panels if necessary to maintain clear cover.
7 Butt adjacent bedding strips together with adhesive. Cut v-notches, approx ½" deep, in the top of the bedding strips at 8' o.c.
8 Equally space additional bar if more than 1'-3" Max.
9 The actual thickness constructed may exceed the slab thickness shown on the Span Details but the extra thickness shall be no more than 2" (1" for Prestressed Concrete U-Beams and Steel Beams). Bearing Seat Elevations or finished grade may be adjusted.
10 Field adjust Bars Z1(#4) to match actual slope of slab overhangs. Width of slab overhang will vary along span with curved slab edges. Adjust Bar Z1(#4) dimensions to maintain proper cover. Bars Z2(#4) are located at Inv-T sheets only.
11 Location of concrete placement sequence boundaries and bolted field splices should be considered by the contractor in determining panel limits.
PLAN AT SPLICE
(Showing Steel Bms with flange width transition)
ELEVATION AT SPLICE
(Showing Steel Bms with different flange thickness)
PRESTRESSED CONCRETE SPREAD SLAB BEAMS
Bars F over exterior beams are still required when no overhang is used. In this case, only one Bar D, 2" from slab edge, is required.
BARS Z (#4) 10
HL93 LOADING
SHEET 2 OF 4
Texas Department of Transportation
Bridge Division
PRESTRESSED CONCRETE PANELS
OPTIONAL DECK DETAILS
PCP

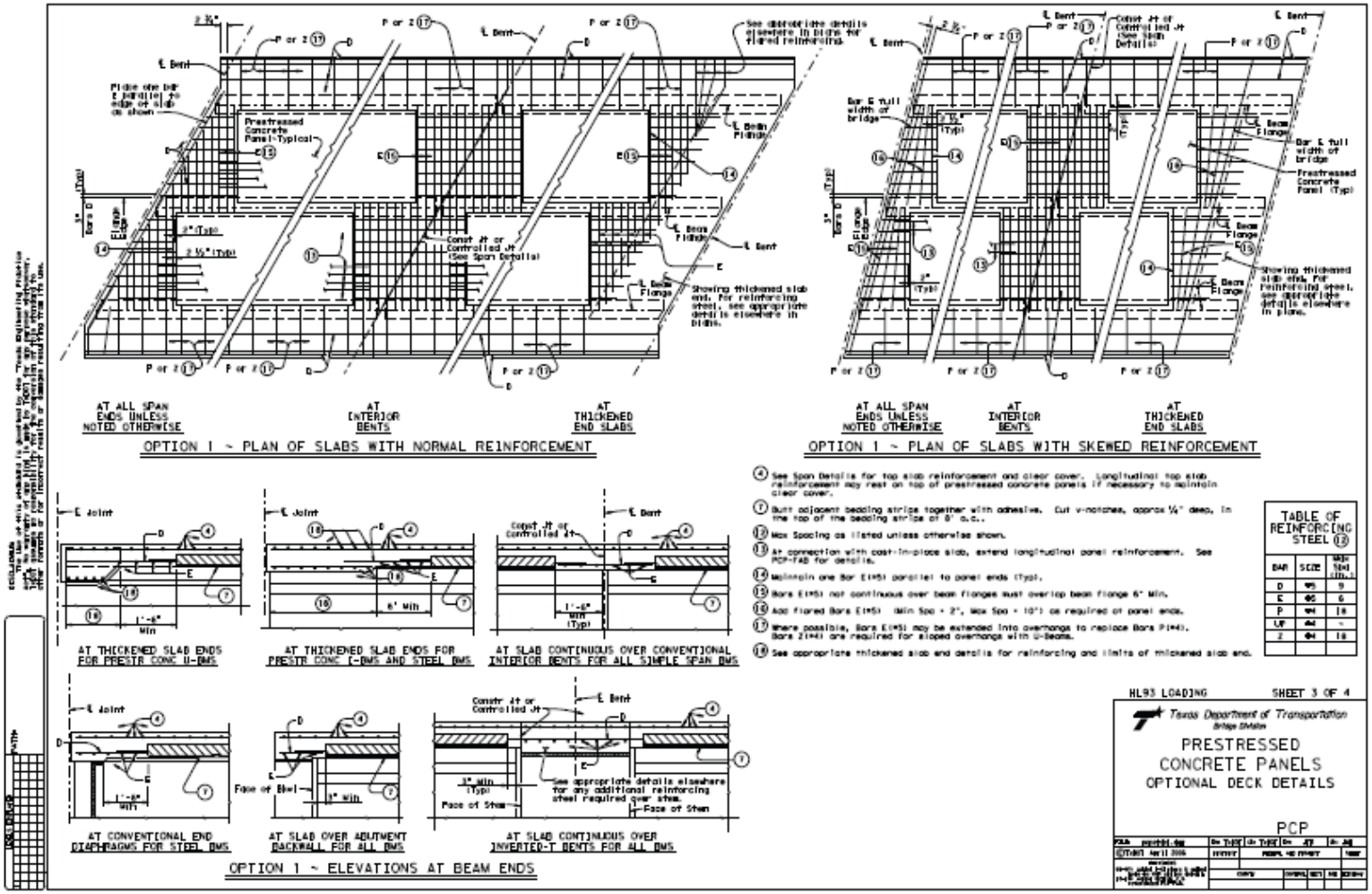
AT ALL SPAN ENDS UNLESS NOTED OTHERWISE
AT INTERIOR BENTS
AT THICKENED END SLABS
OPTION 1 ~ PLAN OF SLABS WITH NORMAL REINFORCEMENT
AT ALL SPAN ENDS UNLESS NOTED OTHERWISE
AT INTERIOR BENTS
AT THICKENED END SLABS
OPTION 1 ~ PLAN OF SLABS WITH SKEWED REINFORCEMENT
AT THICKENED SLAB ENDS FOR PRESTR CONC U-BMS
AT THICKENED SLAB ENDS FOR PRESTR CONC I-BMS AND STEEL BMS
AT SLAB CONTINUOUS OVER CONVENTIONAL INTERIOR BENTS FOR ALL SIMPLE SPAN BMS
AT CONVENTIONAL END DIAPHRAGMS FOR STEEL BMS
AT SLAB OVER ABUTMENT BACKWALL FOR ALL BMS
AT SLAB CONTINUOUS OVER INVERTED-T BENTS FOR ALL BMS
OPTION 1 ~ ELEVATIONS AT BEAM ENDS
TABLE OF REINFORCING STEEL (12)
BAR SIZE
D #5 9
E #6 6
P #4 18
LF #4 -
Z #4 18
HL93 LOADING
SHEET 3 OF 4
Texas Department of Transportation
Bridge Division
PRESTRESSED CONCRETE PANELS
OPTIONAL DECK DETAILS
PCP

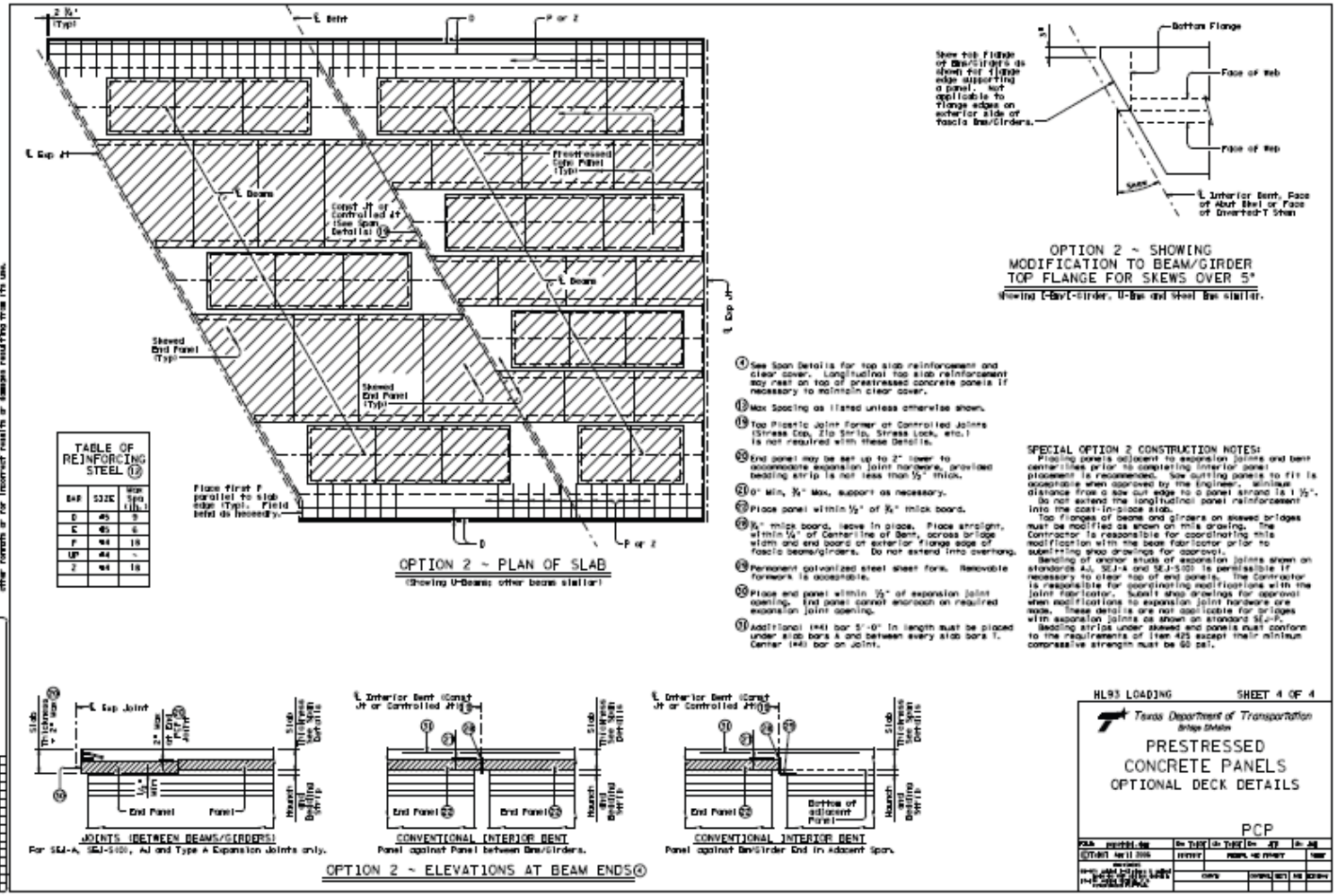
2 ½" (Typ)
℄ Bent
D
P or Z
℄ Exp Jt
Prestressed Conc Panel (Typ)
℄ Beams
Const Jt or Controlled Jt (See Span Details) (19)
Skewed End Panel (Typ)
Place first P parallel to slab edge (Typ). Field bend as necessary.
TABLE OF REINFORCING STEEL (12)
BAR | SIZE | Max Spa c/c in.
D | #5 | 9
E | #5 | 6
F | #4 | 18
LP | #4 | -
Z | #4 | 18
OPTION 2 ~ PLAN OF SLAB
(Showing U-Beams; other beam similar)
Bottom Flange
Face of Web
Face of Web
Skew Sub Fillet at Beam/Girders as shown for flange edge supporting a panel. Not applicable to flange edges on exterior side of fascia Bms/Girders.
℄ Interior Bent, Face of Abut Bwl or Face of Diverted-T Stem
OPTION 2 ~ SHOWING MODIFICATION TO BEAM/GIRDER TOP FLANGE FOR SKEWS OVER 5°
Showing I-Bwl-Girder, U-Bm and Steel Bm similar.
(4) See Span Details for top slab reinforcement and clear cover. Longitudinal top slab reinforcement may rest on top of prestressed concrete panels if necessary to maintain clear cover.
(12) Max Spacing as listed unless otherwise shown.
(19) Top Plastic Joint Former at Controlled Joints (Stress Cap, Zip Strip, Stress Lock, etc.) is not required with these Details.
(20) End panel may be set up to 2" lower to accommodate expansion joint hardware, provided bedding strip is not less than ½" thick.
(21) 0" Min, ¾" Max, support as necessary.
(22) Place panel within ½" of ¾" thick board.
(23) ¾" thick board, leave in place. Place straight, within ¼" of Centerline of Bent, across bridge width and end board at exterior flange edge of fascia beams/girders. Do not extend into overhang.
(24) Permanent galvanized steel sheet form. Removable formwork is acceptable.
(25) Place end panel within ½" of expansion joint opening. End panel cannot encroach on required expansion joint opening.
(27) Additional (#4) bar 5'-0" in length must be placed under slab bars A and between every slab bars T. Center (#4) bar on joint.
SPECIAL OPTION 2 CONSTRUCTION NOTES:
Placing panels adjacent to expansion joints and bent centerlines prior to completing interior panel placement is recommended. Saw cutting panels to fit is acceptable when approved by the Engineer, minimum distance from a saw cut edge to a panel strand is 1 ½".
Do not extend the longitudinal panel reinforcement into the cast-in-place slab.
Top flanges of beams and girders on skewed bridges must be modified as shown on this drawing. The Contractor is responsible for coordinating this modification with the beam fabricator prior to submitting shop drawings for approval.
Bending of anchor studs of expansion joints shown on standards A.J. SEJ-A and SEJ-S100 is permissible if necessary to clear top of end panels. The Contractor is responsible for coordinating modifications with the joint fabricator. Submit shop drawings for approval when modifications to expansion joint hardware are made. These details are not applicable for bridges with expansion joints as shown on standard SEJ-P.
Bedding strips under skewed end panels must conform to the requirements of Item 425 except their minimum compressive strength must be 60 psi.
JOINTS (BETWEEN BEAMS/GIRDERS)
For SEJ-A, SEJ-S100, AJ and Type A Expansion Joints only.
CONVENTIONAL (INTERIOR BENT
Panel against Panel between Bms/Girders.
CONVENTIONAL INTERIOR BENT
Panel against Bm/Girder End in Adjacent Span.
OPTION 2 ~ ELEVATIONS AT BEAM ENDS(4)
HL93 LOADING
SHEET 4 OF 4
Texas Department of Transportation
Bridge Division
PRESTRESSED CONCRETE PANELS
OPTIONAL DECK DETAILS
PCP

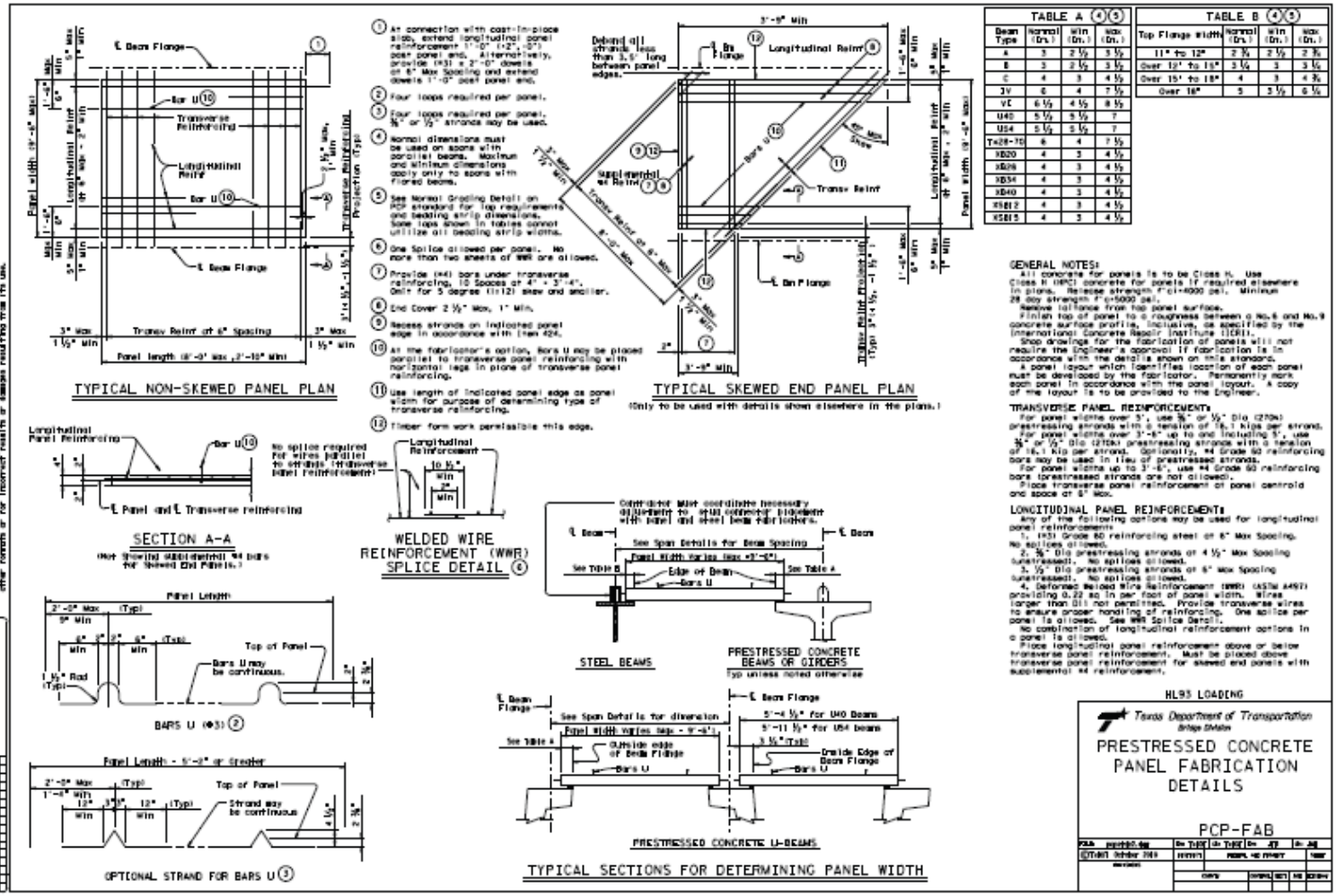

TABLE A ④⑤			
Beam Type	Normal (Dn.)	min (Dn.)	max (Dn.)
A	3	2 ½	5 ½
B	3	2 ½	5 ½
C	4	3	6 ½
3V	6	4	7 ½
VI	6 ½	4 ½	8 ½
U40	5 ½	5 ½	7
U54	5 ½	5 ½	7
T×28-12	6	4	7 ½
XB20	4	3	6 ½
XB28	4	3	6 ½
XB34	4	3	6 ½
XB40	4	3	6 ½
XSB12	4	3	6 ½
XSB15	4	3	6 ½

TABLE B ④⑤			
Top Flange Width	Normal (Dn.)	min (Dn.)	max (Dn.)
11" to 12"	2 ¾	2 ½	2 ¾
Over 12" to 15"	3 ¼	3	3 ½
Over 15" to 18"	4	3	4 ¾
Over 18"	5	3 ½	6 ½

GENERAL NOTES:

All concrete for panels is to be Class H. Use Class H (HPC) concrete for panels if required elsewhere in plans. Release strength f'ci=4000 psi. Minimum 28 day strength f'c=5000 psi.

Remove laitance from top panel surface.

Finish top of panel to a roughness between a No.6 and No.9 concrete surface profile, inclusive, as specified by the (International) Concrete Repair Institute (ICRI).

Shop drawings for the fabrication of panels will not require the Engineer's approval if fabrication is in accordance with the details shown on this standard.

A panel layout which identifies location of each panel must be developed by the fabricator. Permanently mark each panel in accordance with the panel layout. A copy of the layout is to be provided to the Engineer.

TRANSVERSE PANEL REINFORCEMENT:

For panel widths over 3', use ⅜" or ½" Dia (270k) prestressing strands with a tension of 18.1 kips per strand.

For panel widths over 3'-6" up to and including 5', use ⅜" or ½" Dia (270k) prestressing strands with a tension of 18.1 kip per strand. Optionally, #4 Grade 60 reinforcing bars may be used in lieu of prestressed strands.

For panel widths up to 3'-6", use #4 Grade 60 reinforcing bars (prestressed strands are not allowed).

Place transverse panel reinforcement at panel centroid and space at 8" Max.

LONGITUDINAL PANEL REINFORCEMENT:

Any of the following options may be used for longitudinal panel reinforcement:

1. (#3) Grade 60 reinforcing steel at 8" Max Spacing. No splices allowed.
2. ⅜" Dia prestressing strands at 4 ½" Max Spacing (unstressed). No splices allowed.
3. ½" Dia prestressing strands at 8" Max Spacing (unstressed). No splices allowed.
4. Deformed Welded Wire Reinforcement (WWR) (ASTM A497) providing 0.22 sq in per foot of panel width. Wires larger than D11 not permitted. Provide transverse wires to ensure proper handling of reinforcing. One splice per panel is allowed. See WWR Splice Detail.

No combination of longitudinal reinforcement options in a panel is allowed.

Place longitudinal panel reinforcement above or below transverse panel reinforcement. Must be placed above transverse panel reinforcement for skewed end panels with supplemental #4 reinforcement.

HL93 LOADING

Texas Department of Transportation
Bridge Division

PRESTRESSED CONCRETE PANEL FABRICATION DETAILS

PCP-FAB

FILE: pcpfab01.dgn	DN: TxDOT	CK: TxDOT	DW: JTF	CK: AHJ
©TxDOT October 2001	REVISIONS			

A.2 GAGES

A.2.1 PMFL-60

Information about specifications of gage PMFL-60 from Tokyo Sokki Kenkyujyo Co., Ltd. is presented in this section.

TML STRAIN GAUGE TEST DATA

GAUGE TYPE : PMFL-60		TESTTED ON : SS400	
LOT NO. : P515615		COEFFICIENT OF THERMAL EXPANSION : 11.8	$\times 10^{-6}$/℃
GAUGE FACTOR : 2.11	±1%	DATA NO. : V0011	

THERMAL OUTPUT (ε app : APPARENT STRAIN)

$\varepsilon app = 2.35\times10^{-1}+9.16\times10^{-1}\times T^{1}-5.11\times10^{-2}\times T^{2}+2.36\times10^{-4}\times T^{3}$ (μm/m)

TOLERANCE : ±1.8 [(μm/m)/℃], T : TEMPERATURE

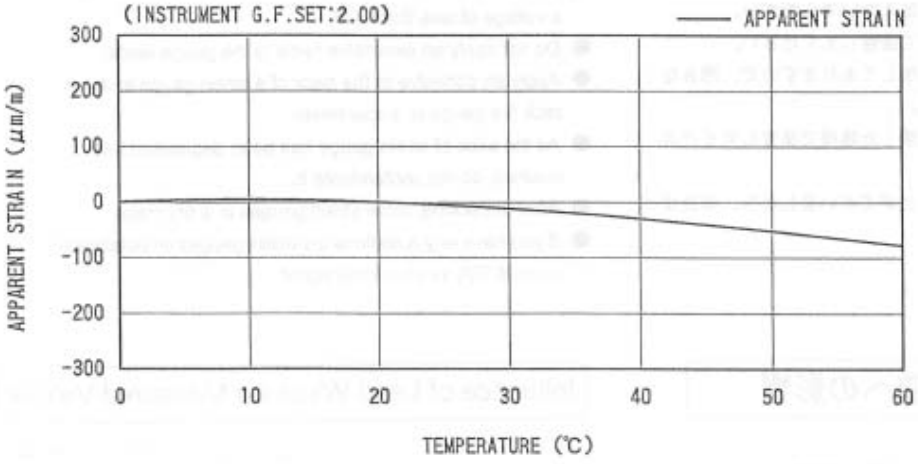

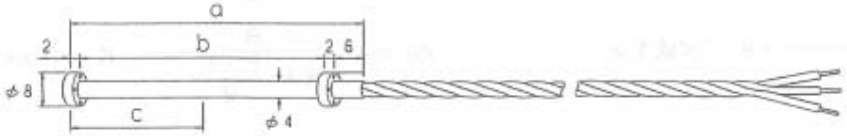

GAUGE TYPE	a	b	c
PMFL-50	60	50	27
PMFL-60	70	60	32

(Unit:mm)

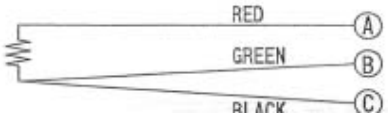

A.2.2 Geokon Model 4200

Information about specifications, theory of operation, thermistor temperature derivation, and high-temperature thermistor linearization of vibrating wire gage Model 4200 from Geokon is presented in this section.

APPENDIX A - SPECIFICATIONS

A.1 Strain Gage

Model:	4200/4200 HT	4202	4204	4210	4212	4214
Range (nominal):	3000 με					
Resolution:	1.0 με[1]	0.4 με[1]	1.0 με[1]	0.4 με[1]	0.4 με[1]	0.4 με[1]
Calibration Accuracy	0.1%FSR					
Typical Batch Factor	0.98	0.91		0.95		
Batch Factor Accuracy	0.5%FSR					
Sytem Accuracy:	2.0% FSR[2]					
Stability:	0.1%FS/yr					
Linearity:	2.0% FSR					
Thermal Coefficient:	12.2 με/°C [3]					
Frequency Range Hz:	450-1200	1400-3500	800-1600	1400-3500	1400-3500	1400-3500
Dimensions (gage): (Length × Diameter)	6.125 × 0.750" 155 × 19 mm	2.250 × 0.625" 57 × 16 mm	4.125 × 0.750" 105 × 19 mm	10.250 × 2" 260 × 50 mm	12.250 × 2" 311 × 50 mm	14.250 × 2" 362 × 50 mm
Dimensions (coil):	0.875 × 0.875" 22 × 22 mm	NA				
Coil Resistance:	180 Ω	50 Ω	50 Ω	180 Ω	180 Ω	180 Ω
Temperature Range:	-20 to +80° C					

Table A-1 Strain Gage Specifications

Notes:
[1] Depends on the readout; figures in Table A-1 pertain to the GK-401 Readout.
[2] System Accuracy takes into account hysteresis, non-linearity, misalignment, batch factor variations, and other aspects of the actual measurement program. System Accuracy to 1.0% FS may be achieved through individual calibration of each strain gage.
[3] The Model 4200HT high temperature strain gage has a Thermal Coefficient of 17.3 με/°C

A.2 Thermistor (see Appendix C also)

Range: -80 to +150° C
Accuracy: ±0.5° C

APPENDIX B - THEORY OF OPERATION

A vibrating wire attached to the surface of a deforming body will deform in a like manner. The deformations alter the tension of the wire and hence also it's natural frequency of vibration (resonance). The relationship between frequency (period) and deformation (strain) is described as follows:

Model:	4200/4200HT	4202	4204
Gage Length (L_g):	6.000 inches	2 inches	4.000 inches
Wire Length (L_W):	5.875 inches	2 inches	3.875 inches
Gage Factor:	3.304	0.391	1.422

Table B-1 - Embedment Strain Gage Theoretical Parameters

Note: The examples below are calculated using the Model 4200 gage parameters. Substitute the values from Table B-1 for the Models 4202/4204 strain gages. **These equations do not apply to the Models-4202X/4210/4212/4214 strain gages.**

1. The fundamental frequency (resonant frequency) of vibration of a wire is related to its tension, length and mass by the equation: $$f = \frac{1}{2L_w}\sqrt{\frac{F}{m}}$$

Where;
L_w is the length of the wire in inches.
F is the wire tension in pounds.
m is the mass of the wire per unit length (pounds, sec.^{2}/in.^{2}).

2. Note that: $$m = \frac{W}{L_w g}$$

Where;
W is the weight of L_w inches of wire (pounds).
g is the acceleration of gravity (386 in./sec.^{2}).

3. and: $$W = \rho a L_w$$

Where;
ρ is the wire material density (0.283 lb./in.^{3}).
a is the cross sectional area of the wire (in.^{2}).

4. Combining equations 1, 2 and 3 gives: $$f = \frac{1}{2L_w}\sqrt{\frac{Fg}{\rho a}}$$

5. Note that the tension (F) can be expressed in terms of strain, e.g.:

$$F = \varepsilon_w E a$$

Where;
ε_w is the wire strain (in./in.).
E is the Young's Modulus of the wire (30 x 10^6 Psi).

6. Combining equations 4 and 5 gives:

$$f = \frac{1}{2L_w}\sqrt{\frac{\varepsilon_w E g}{\rho}}$$

7. Substituting the given values for E, g and ρ yields:

$$f = \frac{101142}{L_w}\sqrt{\varepsilon_w}$$

8. On channel 'A', which displays the period of vibration, T, multiplied by a factor of 10^6:

$$T = \frac{10^6}{f}$$

9. Combining equations 7 and 8 gives:

$$\varepsilon_w = \frac{97.75 L_w^{\ 3}}{T^2}$$

10. Equation 9 must now be expressed in terms of the strain in the surface of the body to which the gage is attached. Since the deformation of the body must equal the deformation of the wire:

$$\varepsilon_w L_w = \varepsilon L_g$$

Where;
ε is the strain in the body.
L_g is the gage length (in inches).

11. Combining equations 9 and 10 gives:

$$\varepsilon = \frac{97.75}{T^2} \cdot \frac{L_w^{\ 3}}{L_g}$$

Where; (for the VCE-4200 Strain Gage)
L_w is 5.875 inches.
L_g is 6.000 inches.

12. Therefore: $$\varepsilon = 3.304 \times 10^3 [\frac{1}{T^2}]$$

(Note that T is in seconds x 10^6 and ε is in inches per inch)

13. The display on position "D" of the GK-401/403 Readout is based on the equation:

$$\varepsilon = 3.304 \times 10^9 [\frac{1}{T^2}]$$

Note that in this formula ε is in micro inches per inch and T is in seconds x 10^6

Alternatively $\varepsilon = 3.304 \times 10^{-3} f^2$ microstrain. Where f is the frequency in Hz

The squaring, inverting and multiplication by the factor, 3.304×10^9, is all done internally by the microprocessor so that the displayed reading on Channel D is given in terms of microinches per inch (ε).

APPENDIX C - THERMISTOR TEMPERATURE DERIVATION

Thermistor Type: YSI 44005, Dale #1C3001-B3, Alpha #13A3001-B3

Resistance to Temperature Equation:

$$T = \frac{1}{A + B(LnR) + C(LnR)^3} - 273.2$$

Equation C-1 Convert Thermistor Resistance to Temperature

Where: T = Temperature in °C.
LnR = Natural Log of Thermistor Resistance
A = 1.4051×10^{-3} (coefficients calculated over the −50 to +150° C. span)
B = 2.369×10^{-4}
C = 1.019×10^{-7}

Ohms	Temp	Ohms	Temp	Ohms	Temp	Ohms	Temp	Ohms	Temp
201.1K	-50	16.60K	-10	2417	+30	525.4	+70	153.2	+110
187.3K	-49	15.72K	-9	2317	31	507.8	71	149.0	111
174.5K	-48	14.90K	-8	2221	32	490.9	72	145.0	112
162.7K	-47	14.12K	-7	2130	33	474.7	73	141.1	113
151.7K	-46	13.39K	-6	2042	34	459.0	74	137.2	114
141.6K	-45	12.70K	-5	1959	35	444.0	75	133.6	115
132.2K	-44	12.05K	-4	1880	36	429.5	76	130.0	116
123.5K	-43	11.44K	-3	1805	37	415.6	77	126.5	117
115.4K	-42	10.86K	-2	1733	38	402.2	78	123.2	118
107.9K	-41	10.31K	-1	1664	39	389.3	79	119.9	119
101.0K	-40	9796	0	1598	40	376.9	80	116.8	120
94.48K	-39	9310	+1	1535	41	364.9	81	113.8	121
88.46K	-38	8851	2	1475	42	353.4	82	110.8	122
82.87K	-37	8417	3	1418	43	342.2	83	107.9	123
77.66K	-36	8006	4	1363	44	331.5	84	105.2	124
72.81K	-35	7618	5	1310	45	321.2	85	102.5	125
68.30K	-34	7252	6	1260	46	311.3	86	99.9	126
64.09K	-33	6905	7	1212	47	301.7	87	97.3	127
60.17K	-32	6576	8	1167	48	292.4	88	94.9	128
56.51K	-31	6265	9	1123	49	283.5	89	92.5	129
53.10K	-30	5971	10	1081	50	274.9	90	90.2	130
49.91K	-29	5692	11	1040	51	266.6	91	87.9	131
46.94K	-28	5427	12	1002	52	258.6	92	85.7	132
44.16K	-27	5177	13	965.0	53	250.9	93	83.6	133
41.56K	-26	4939	14	929.6	54	243.4	94	81.6	134
39.13K	-25	4714	15	895.8	55	236.2	95	79.6	135
36.86K	-24	4500	16	863.3	56	229.3	96	77.6	136
34.73K	-23	4297	17	832.2	57	222.6	97	75.8	137
32.74K	-22	4105	18	802.3	58	216.1	98	73.9	138
30.87K	-21	3922	19	773.7	59	209.8	99	72.2	139
29.13K	-20	3748	20	746.3	60	203.8	100	70.4	140
27.49K	-19	3583	21	719.9	61	197.9	101	68.8	141
25.95K	-18	3426	22	694.7	62	192.2	102	67.1	142
24.51K	-17	3277	23	670.4	63	186.8	103	65.5	143
23.16K	-16	3135	24	647.1	64	181.5	104	64.0	144
21.89K	-15	**3000**	**25**	624.7	65	176.4	105	62.5	145
20.70K	-14	2872	26	603.3	66	171.4	106	61.1	146
19.58K	-13	2750	27	582.6	67	166.7	107	59.6	147
18.52K	-12	2633	28	562.8	68	162.0	108	58.3	148
17.53K	-11	2523	29	543.7	69	157.6	109	56.8	149
								55.6	150

Table C-1 Thermistor Resistance versus Temperature

APPENDIX D - HIGH-TEMPERATURE THERMISTOR LINEARIZATION

High Temperature Thermistor Linearization using SteinHart-Hart Log Equation

Thermistor Type: Thermometrics BR55KA822J

Basic Equation: $$T = \frac{1}{A + B(LnR) + C(LnR)^3} - 273.2$$

Where:
T = Temperature in °C
LnR = Natural Log of Thermistor Resistance
$A = 1.02569 \times 10^{-3}$
$B = 2.478265 \times 10^{-4}$
$C = 1.289498 \times 10^{-7}$

Note: Coefficients calculated over -30° to +260° C. span.

Temperature Calculation and Error Table

Temp	R (ohms)	LnR	LnR^3	Calculated Temp	Diff	FS Error	Temp	R (ohms)	LnR	LnR^3	Calculated Temp	Diff	FS Error
-30	113898	11.643	1578.342	-30.17	0.17	0.06	120	407.62	6.010	217.118	120.00	0.00	0.00
-25	86182	11.364	1467.637	-25.14	0.14	0.05	125	360.8	5.888	204.162	125.00	0.00	0.00
-20	65805	11.094	1365.581	-20.12	0.12	0.04	130	320.21	5.769	191.998	130.00	0.00	0.00
-15	50684.2	10.833	1271.425	-15.10	0.10	0.03	135	284.95	5.652	180.584	135.00	0.00	0.00
-10	39360	10.581	1184.457	-10.08	0.08	0.03	140	254.2	5.538	169.859	140.01	-0.01	0.00
-5	30807.4	10.336	1104.068	-5.07	0.07	0.02	145	227.3	5.426	159.773	145.02	-0.02	-0.01
0	24288.4	10.098	1029.614	-0.05	0.05	0.02	150	203.77	5.317	150.314	150.03	-0.03	-0.01
5	19294.6	9.868	960.798	4.96	0.04	0.01	155	183.11	5.210	141.428	155.04	-0.04	-0.01
10	15424.2	9.644	896.871	9.98	0.02	0.01	160	164.9	5.105	133.068	160.06	-0.06	-0.02
15	12423	9.427	837.843	14.98	0.02	0.01	165	148.83	5.003	125.210	165.08	-0.08	-0.03
20	10061.4	9.216	782.875	19.99	0.01	0.00	170	134.64	4.903	117.837	170.09	-0.09	-0.03
25	8200	9.012	731.893	25.00	0.00	0.00	175	122.1	4.805	110.927	175.08	-0.08	-0.03
30	6721.54	8.813	684.514	30.01	-0.01	0.00	180	110.95	4.709	104.426	180.07	-0.07	-0.02
35	5540.74	8.620	640.478	35.01	-0.01	0.00	185	100.94	4.615	98.261	185.10	-0.10	-0.04
40	4592	8.432	599.519	40.02	-0.02	-0.01	190	92.086	4.523	92.512	190.09	-0.09	-0.03
45	3825.3	8.249	561.392	45.02	-0.02	-0.01	195	84.214	4.433	87.136	195.05	-0.05	-0.02
50	3202.92	8.072	525.913	50.01	-0.01	-0.01	200	77.088	4.345	82.026	200.05	-0.05	-0.02
55	2693.7	7.899	492.790	55.02	-0.02	-0.01	205	70.717	4.259	77.237	205.02	-0.02	-0.01
60	2276.32	7.730	461.946	60.02	-0.02	-0.01	210	64.985	4.174	72.729	210.00	0.00	0.00
65	1931.92	7.566	433.157	65.02	-0.02	-0.01	215	59.819	4.091	68.484	214.97	0.03	0.01
70	1646.56	7.406	406.283	70.02	-0.02	-0.01	220	55.161	4.010	64.494	219.93	0.07	0.02
75	1409.58	7.251	381.243	75.01	-0.01	0.00	225	50.955	3.931	60.742	224.88	0.12	0.04
80	1211.14	7.099	357.808	80.00	0.00	0.00	230	47.142	3.853	57.207	229.82	0.18	0.06
85	1044.68	6.951	335.915	85.00	0.00	0.00	235	43.673	3.777	53.870	234.77	0.23	0.08
90	903.64	6.806	315.325	90.02	-0.02	-0.01	240	40.533	3.702	50.740	239.69	0.31	0.11
95	785.15	6.666	296.191	95.01	-0.01	0.00	245	37.671	3.629	47.788	244.62	0.38	0.13
100	684.37	6.528	278.253	100.00	0.00	0.00	250	35.055	3.557	45.001	249.54	0.46	0.16
105	598.44	6.394	261.447	105.00	0.00	0.00	255	32.677	3.487	42.387	254.44	0.56	0.19
110	524.96	6.263	245.705	110.00	0.00	0.00	260	30.496	3.418	39.917	259.34	0.66	0.23
115	461.91	6.135	230.952	115.00	0.00	0.00							

Table B-2: High Temperature Thermistor Resistance versus Temperature.

A.3 AASHTO PRESTRESS LOSS PREDICTIONS FOR CURRENT INITIAL PRESTRESS

Prestress loss predictions based on AASHTO provisions for the panels fabricated with current initial prestress (16.1 kips/strand).

A3.1 2004 AASHTO

Gross Section Properties	
h [in]	4
y_t [in]	2
y_b [in]	2
A_g [in^2]	384
I_g [in^4]	512
p_s [in]	200
w_{sw} [klf]	400
e_{cl} [in]	0.00
e_{end} [in]	0.00
A_{ps} [in^2]	1.36
y_s [in]	2.06
A_s [in^2]	0.62

Strand Stresses	
f_{pj} [ksi]	189.41
P_j [kips]	257.6
f_{po} [ksi]	184.3
P_o [kips]	250.7

Concrete Age	
t_i [days]	1
t_f [days]	100000

Span Properties	
L_{span} [ft]	6
L_{beam} [ft]	8
$M_{g,\ span}$ [kin]	21600.0
$M_{g,\ beam}$ [kin]	38400

Material Properties	
n	7.6
n_{LT}	6.8
Concrete	
f'_{ci} [ksi]	4
E_{ci} [ksi]	3739
f'_c [ksi]	5
E_c [ksi]	4180
w_c [kcf]	0.1475
Strand	
f_{pu} [ksi]	270
f_{py} [ksi]	243
E_p [ksi]	28500

Total Loss

$$\Delta f_{pT} = \Delta f_{pES} + \Delta f_{pSR} + \Delta f_{pCR} + \Delta f_{pR2}$$

Δf_{pT} [ksi]	24.2
Δf_{pES} [ksi]	5.1
Δf_{pSR} [ksi]	6.5
Δf_{pCR} [ksi]	8.0
Δf_{pR2} [ksi]	4.5

Elastic Shortening

$$\Delta f_{pES} = \frac{E_p}{E_{ci}} f_{cgp}$$

$$f_{cgp} = 0.7 f_{pu} A_{ps} \left(\frac{1}{A_g} + \frac{e_{cl}^2}{I_g} \right) - \frac{M_{g,beam} e_{cl}}{I_g}$$

Δf_{pES} [ksi]	5.1
f_{cgp} [ksi]	0.7

Shrinkage

$$\Delta f_{pSR} = 17.0 - 0.150H$$

Δf_{pSR} [ksi]	6.5
H [%]	70

Creep

$$\Delta f_{pCR} = 12.0 f_{cgp} - 7.0 \Delta f_{cdp} \geq 0$$

Δf_{pCR} [ksi]	8.0
f_{cgp} [ksi]	0.7
Δf_{cdp} [ksi]	0.0

Relaxation

$$\Delta f_{pR2} = \frac{3}{10} [20 - 0.4 \Delta f_{pES} - 0.2(\Delta f_{pSR} + \Delta f_{pCR})]$$

Δf_{pR2} [ksi]	4.5

A3.2 2008 AASHTO

Gross Section Properties	
h [in]	4
y_t [in]	2
y_b [in]	2
A_g [in^2]	384
I_g [in^4]	512
p_s [in]	200
w_{sw} [klf]	400
e_{cl} [in]	0.00
e_{end} [in]	0.00
A_{ps} [in^2]	1.36
y_s [in]	2.06
A_s [in^2]	0.62

Strand Stresses	
f_{pj} [ksi]	189.4
P_j [kips]	257.6
f_{po} [ksi]	184.4
P_o [kips]	250.8

Concrete Age	
t_i [days]	1
t_f [days]	100000

Span Properties	
L_{span} [ft]	8
L_{beam} [ft]	8
$M_{g,\ span}$ [kin]	38400.0
$M_{g,\ beam}$ [kin]	38400

Material Properties	
n	7.6
n_{LT}	6.8
Concrete	
f'_{ci} [ksi]	4
E_{ci} [ksi]	3739
f'_c [ksi]	5
E_c [ksi]	4180
w_c [kcf]	0.1475
K_1	1.0
Strand	
f_{pu} [ksi]	270
f_{py} [ksi]	243
E_p [ksi]	28500

Total Loss

$$\Delta f_{pT} = \Delta f_{pES} + \Delta f_{pLT}$$

$$\Delta f_{pLT} = \left(\Delta f_{pSR} + \Delta f_{pCR} + \Delta f_{pR1}\right)_{id}$$

Δf_{pT} [ksi]	34.0
Δf_{pES} [ksi]	5.0
Δf_{pSR} [ksi]	15.8
Δf_{pCR} [ksi]	10.7
Δf_{pR} [ksi]	2.6

Elastic Shortening

$$\Delta f_{pES} = \frac{A_{ps} f_{pbt}\left(I_g + e_{ci}^2 A_g\right) - e_{ci} M_g A_g}{A_{ps}\left(I_g + e_{ci}^2 A_g\right) + \frac{A_g I_g E_{ci}}{E_p}}$$

Δf_{pES} [ksi]	5.0
f_{pbt} [ksi]	189.4

Shrinkage

$$\Delta f_{pSR} = \varepsilon_{bid} E_p K_{id}$$

$$\varepsilon_{bid} = k_s k_{hs} k_f k_{td} (0.48 \cdot 10^{-3})$$

$$K_{id} = \frac{1}{1 + \frac{E_p}{E_{ci}} \frac{A_{ps}}{A_g}\left(1 + \frac{A_g e_{ci}^2}{I_g}\right)\left[1 + 0.7\psi_B(t_f, t_i)\right]}$$

$$\psi_B(t_f, t_i) = 1.9 k_s k_{hc} k_{td} t_i^{-0.118}$$

$$k_s = 1.45 - 0.13\frac{V}{S}$$

$$k_{hs} = 2.00 - 0.014H \qquad k_{hc} = 1.56 - 0.008H$$

$$k_f = \frac{5}{1 + f'_{ci}} \qquad k_{td} = \frac{(t_f - t_i)}{61 - 4f'_{ci} + (t_f - t_i)}$$

Δf_{pSR} [ksi]	15.8
ε_{bid} [in/in]	0.0006
k_s	1.21
k_{hs}	1.02
k_f	1.00
k_{td}	1.00
V/S	1.8
H [%]	70
K_{id}	0.9
$\Psi_b(t_f,t_i)$	2.3
k_{hc}	1.00

Creep

$$\Delta f_{pCR} = \frac{E_p}{E_{ci}} f_{cgp} \psi_b(t_f, t_i) K_{id}$$

Δf_{pCR} [ksi]	10.7
f_{cgp} [ksi]	0.7

Relaxation

$$\Delta f_{pR1} = \frac{f_{pt}}{K_L}\left(\frac{f_{pt}}{f_{py}} - 0.55\right)$$

$$\Delta f_{pR2} = \Delta f_{pR1}$$

Δf_{pR1} [ksi]	1.3
f_{pt} [ksi]	184
K_L	30
Δf_{pR2} [ksi]	1.3

A.4 AASHTO PRESTRESS LOSS PREDICTIONS FOR LOWER INITIAL PRESTRESS

Prestress loss predictions based on AASHTO provisions for the panels fabricated with proposed lower initial prestress (14.4 kips/strand).

A4.1 2004 AASHTO

Gross Section Properties	
h [in]	4
y_t [in]	2
y_b [in]	2
A_g [in^2]	384
I_g [in^4]	512
p_s [in]	200
w_{sw} [klf]	400
e_{cl} [in]	0.00
e_{end} [in]	0.00
A_{ps} [in^2]	1.36
y_s [in]	2.06
A_s [in^2]	0.62

Strand Stresses	
f_{pj} [ksi]	169.41
P_j [kips]	230.4
f_{po} [ksi]	164.3
P_o [kips]	223.5

Concrete Age	
t_i [days]	1
t_f [days]	100000

Span Properties	
L_{span} [ft]	6
L_{beam} [ft]	8
$M_{g,\,span}$ [kin]	21600.0
$M_{g,\,beam}$ [kin]	38400

Material Properties	
n	7.6
n_{LT}	6.8
Concrete	
f'_{ci} [ksi]	4
E_{ci} [ksi]	3739
f'_c [ksi]	5
E_c [ksi]	4180
w_c [kcf]	0.1475
Strand	
f_{pu} [ksi]	270
f_{py} [ksi]	243
E_p [ksi]	28500

Total Loss

$$\Delta f_{pT} = \Delta f_{pES} + \Delta f_{pSR} + \Delta f_{pCR} + \Delta f_{pR2}$$

Δf_{pT} [ksi]	24.2
Δf_{pES} [ksi]	5.1
Δf_{pSR} [ksi]	6.5
Δf_{pCR} [ksi]	8.0
Δf_{pR2} [ksi]	4.5

Elastic Shortening

$$\Delta f_{pES} = \frac{E_p}{E_{ci}} f_{cgp}$$

$$f_{cgp} = 0.7 f_{pu} A_{ps} \left(\frac{1}{A_g} + \frac{e_{cl}^2}{I_g} \right) - \frac{M_{g,beam} e_{cl}}{I_g}$$

Δf_{pES} [ksi]	5.1
f_{cgp} [ksi]	0.7

Shrinkage

$$\Delta f_{pSR} = 17.0 - 0.150H$$

Δf_{pSR} [ksi]	6.5
H [%]	70

Creep

$$\Delta f_{pCR} = 12.0 f_{cgp} - 7.0 \Delta f_{cpd} \geq 0$$

Δf_{pCR} [ksi]	8.0
f_{cgp} [ksi]	0.7
Δf_{cdp} [ksi]	0.0

Relaxation

$$\Delta f_{pR2} = \frac{3}{10} \left[20 - 0.4 \Delta f_{pES} - 0.2 (\Delta f_{pSR} + \Delta f_{pCR}) \right]$$

Δf_{pR2} [ksi]	4.5

A4.2 2008 AASHTO

Gross Section Properties	
h [in]	4
y_t [in]	2
y_b [in]	2
A_g [in^2]	384
I_g [in^4]	512
p_s [in]	200
w_{sw} [klf]	400
e_{cl} [in]	0.00
e_{end} [in]	0.00
A_{ps} [in^2]	1.36
y_s [in]	2.06
A_s [in^2]	0.62

Strand Stresses	
f_{pj} [ksi]	169.4
P_j [kips]	230.4
f_{po} [ksi]	165.0
P_o [kips]	224.3

Concrete Age	
t_i [days]	1
t_f [days]	100000

Span Properties	
L_{span} [ft]	8
L_{beam} [ft]	8
$M_{g,\,span}$ [kin]	38400.0
$M_{g,\,beam}$ [kin]	38400

Material Properties	
n	7.6
n_{LT}	6.8
Concrete	
f'_{ci} [ksi]	4
E_{ci} [ksi]	3739
f'_c [ksi]	5
E_c [ksi]	4180
w_c [kcf]	0.1475
K_1	1.0
Strand	
f_{pu} [ksi]	270
f_{py} [ksi]	243
E_p [ksi]	28500

Total Loss

$$\Delta f_{pT} = \Delta f_{pES} + \Delta f_{pLT}$$

$$\Delta f_{pLT} = \left(\Delta f_{pSR} + \Delta f_{pCR} + \Delta f_{pR1}\right)_{td}$$

Δf_{pT} [ksi]	31.2
Δf_{pES} [ksi]	4.5
Δf_{pSR} [ksi]	15.8
Δf_{pCR} [ksi]	9.6
Δf_{pR} [ksi]	1.4

Elastic Shortening

$$\Delta f_{pES} = \frac{A_{ps} f_{pbt} \left(I_g + e_{ci}^2 A_g\right) - e_{ci} M_g A_g}{A_{ps}\left(I_g + e_{ci}^2 A_g\right) + \frac{A_g I_g E_{ci}}{E_p}}$$

Δf_{pES} [ksi]	4.5
f_{pbt} [ksi]	169.4

Shrinkage

$$\Delta f_{pSR} = \varepsilon_{bid} E_p K_{id}$$

$$\varepsilon_{bid} = k_s k_{hs} k_f k_{td} (0.48 \cdot 10^{-3})$$

$$K_{id} = \frac{1}{1 + \frac{E_p}{E_{ci}} \frac{A_{ps}}{A_g}\left(1 + \frac{A_g e_{pn}^2}{I_g}\right)\left[1 + 0.7\psi_b(t_f, t_i)\right]}$$

$$\psi_b(t_f, t_i) = 1.9 k_s k_{hc} k_{td} t_i^{-0.118}$$

$$k_s = 1.45 - 0.13\frac{V}{S}$$

$$k_{hs} = 2.00 - 0.014H \qquad k_{hc} = 1.56 - 0.008H$$

$$k_f = \frac{5}{1 + f'_{ci}} \qquad k_{td} = \frac{(t_f - t_i)}{61 - 4f'_{ci} + (t_f - t_i)}$$

Δf_{pSR} [ksi]	15.8
ε_{bid} [in/in]	0.0006
k_s	1.21
k_{hs}	1.02
k_f	1.00
k_{td}	1.00
V/S	1.8
H [%]	70
K_{id}	0.9
$\Psi_b(t_f,t_i)$	2.3
k_{hc}	1.00

Creep

$$\Delta f_{pCR} = \frac{E_p}{E_{ci}} f_{cgp} \psi_b(t_f, t_i) K_{id}$$

Δf_{pCR} [ksi]	9.6
f_{cgp} [ksi]	0.6

Relaxation

$$\Delta f_{pR1} = \frac{f_{pt}}{K_L}\left(\frac{f_{pt}}{f_{py}} - 0.55\right)$$

$$\Delta f_{pR2} = \Delta f_{pR1}$$

Δf_{pR1} [ksi]	0.7
f_{pt} [ksi]	165
K_L	30
Δf_{pR2} [ksi]	0.7

REFERENCES

AASHTO (2004): *LRFD Bridge Design Specifications*, 3rd Edition, American Association of State Highway and Transportation Officials, Washington, D.C.

AASHTO (2005): *LRFD Bridge Design Specifications*, Interim 2005 Edition, American Association of State Highway and Transportation Officials, Washington, D.C.

AASHTO (1975): *Standard Specifications for Highway Bridges*, 11th Edition, American Association of State Highway and Transportation Officials, Washington, D.C.

AASHTO (1961): *Standard Specifications for Highway Bridges*, 8th Edition, American Association of State Highway and Transportation Officials, Washington, D.C.

ACI Committee 209 (1971): "Effects of Concrete Constituents, Environment, and Stress on Creep and Shrinkage of Concrete," *ACI Special Publication SP 27-1*, American Concrete Institute, Farmington Hills, MI.

ACI Committee 209 (1992): *Prediction of Creep, Shrinkage, and Temperature Effects in Concrete Structures*, American Concrete Institute, Farmington Hills, MI.

ACI Committee 318 (2008): *Building Code Requirements for Structural Concrete and Commentary*, American Concrete Institute, Farmington Hills, MI.

ACI-ASCE Committee 323 (1958): "Tentative Recommendations for Prestressed Concrete - Committee Closure," ACI Journal, *Proceedings*, American Concrete Institute, Farmington Hills, MI, No. 54, pp. 1291-1299.

Barker (1975): Barker, J. M., "Research, Application, and Experience with Precast Prestressed Bridge Deck Panels." *PCI Journal*, Precast/Prestressed Concrete Insitute, Chicago, IL, pp. 66-85.

Barnoff *et al.* (1977): Barnoff, R., Orndorff, J., Harbaugh, R., and Rainey, D., "Full Scale Test of a Prestressed Bridge with Precast Deck Panels," *PCI Journal*, Precast/Prestressed Concrete Insitute, Chicago, IL, V. 22, No. 5, Sep.-Oct., pp. 66-82.

Bazant *et al.* (1980): Bazant, Z. P., and Panula, L., "Creep and Shrinkage Characterization for Analyzing Prestressed Concrete Structures." *PCI Journal*, Precast/Prestressed Concrete Insitute, Chicago, IL, May-June, pp. 86-122.

Benítez *et al.* (2011): Benítez, J., and Gálvez, J., “Bond Modeling of Prestressed Concrete During the Prestressing Force Release,” *Materials and Structures*, Springer Netherlands, V. 44, Issue 1, pp. 263-278.

Berwanger *et al.* (1976): Berwanger, C., and Sarkar, A. F., "Thermal Expansion of Concrete and Reinforced Concrete*." ACI Journal*, American Concrete Institute, Farmington Hills, MI, Nov., pp. 618-621.

Emanuel *et al.* (1977): Emanuel, J. H., and Hulsey, J. L., "Prediction of the thermal coefficient of expansion of concrete." *ACI Journal*, American Concrete Institute, Farmington Hills, MI, Apr., pp. 149-155.

Erickson (1957): Erickson, E.L., "The Bureau of Public Roads 'Criteria for Prestressed Concrete Bridges’ (A9-1-A9-8)," *Proceedings*, World Conference on Prestressed Concrete, University of California at Berkeley, San Francisco, CA.

Fang *et al.* (1990): Fang, I.-K., Worley, J., Burns, N. H., and Klingner, R. E., "Behavior of Isotropic R/C Bridge Decks on Steel Girders," *Journal of Structural Engineering*, American Society of Civil Engineers, Reston, VA, V. 116, No. 3, Mar., pp. 659-678.

FIB (2007): *Treatment of Imperfections in Precast Structural Elements*, International Federation for Structural Concrete, Lausanne, Switzerland.

Foreman (2010): Foreman, J, “Controlling Cracking in Prestressed Concrete Panels,” MS Thesis, The University of Texas at Austin, Austin, TX.

Foster (2010): Foster, S, “Reducing Top Mat Reinforcement in Bridge Decks,” MS Thesis, The University of Texas at Austin, Austin, TX.

Galvez *et al.* (2009): Galvez, J. C., Benitez, J. M., Tork, B., Casati, M. J., and Cendron, D. A., "Splitting Failure of Precast Prestressed Concrete During the Release of the Prestressing Force," *Engineering Failure Analysis*, Elsevier, Amsterdam, Netherlands.

Hanson *et al.* (1959): Hanson, N. W., and Kaar, P. R., "Flexural Bond Tests of Pretensioned Prestressed Beams," *ACI Journal*, American Concrete Institute, Farmington Hills, MI, Jan., pp. 783-802.

Hawkins (1981): Hawkins, N. M., "Impact of Research on Prestressed Concrete Specimens," *ACI Journal*, American Concrete Institute, Farmington Hills, MI, pp. 163-176.

Homayoun *et al.* (1993): Homayoun, H. A., and Mitchell, D., "Bond Characteristics of Pretensioned Strand," *ACI Materials Journal*, American Concrete Institute, Farmington Hills, MI, May-June, pp. 228-235.

Hoyer (1939): Hoyer, E., and Friedrich, E., "Beitrag zur frage der Hatspannung in Eisen betonbauteilen (Contribution to the question of bond stress in reinforced concrete elements)," *Beton und Eisen 38*.

Jahangirnejad *et al.* (2010): Jahangirnejad, S., Buch, N., "Comparison of Portland Cement Concrete and CTE Calculation Protocols," *Paving Materials and Pavement Analysis*, GeoShanghai International Conference 2010, American Society of Civil Engineers, Shanghai, China, pp. 176-183.

Janney (1954): Janney, J. R., "Nature of Bond in Pretensioned Prestressed Concrete," *ACI Journal*, American Concrete Institute, Farmington Hills, MI, V. 50, No. 9, pp. 717-769.

Jiang *et al.* (1984): Jiang, D. H., Shah, S. P., and Andonian, A. T., "Study of the Transfer of Tensile Forces by Bond," *ACI Journal*, American Concrete Institute, Farmington Hills, MI, May-June, pp. 251-259.

Jones *et al.* (1970): Jones, H., and Furr, H., "Development Length of Strands in Prestressed Panel Subdecks," Texas Transportation Institute, College Station, TX.

Kreisa (2008): Kreisa, A, "Constructibility of Prestressed Concrete Panels for Use at Skewed," Thesis, The University of Texas at Austin, Austin, TX.

Martin *et al.* (1976): Martin, L. D., and Scott, N. L., "Development of Prestressing Strand in Pretensioned Members," *ACI Journal*, American Concrete Institute, Farmington Hills, MI, Aug., pp. 453-456.

Marti-Vargas *et al.* (2007): Marti-Vargas, J. R., Arbelaez, C. A., Serna-Ros, P., and Castro-Bugallo, C., "Reliability of Transfer Length Estimation from Strand End Slip," *ACI Structural Journal*, American Concrete Institute, Farmington Hills, MI, July-Aug., pp. 487-494.

Marti-Vargas *et al*. (2012): Marti-Vargas, J.R., Serna, P., Navarro-Gregori, J., and Bonet, J.L., "Effect of Concrete Composition on Transmission Length of Prestressing Strands," *Construction and Building Materials*, Elsevier, Amsterdam, Netherlands, Vol. 27, Issue 1, pp. 350-356.

Merrill (2002): Merrill, B. D., "Texas' Use of Precast Concrete Stay-In-Place Forms for Bridge Decks," *Proceedings*, Concrete Bridge Conference, National Concrete Bridge Council, Skokie, IL.

Mitchell *et al.* (1993): Mitchell, D., Cook, W. D., Khan, A. A., and Tham, T., "Influence of High Strength Concrete on Transfer and Development Length of Pretensioning Strands," *PCI Journal*, Precast/Prestressed Concrete Insitute, Chicago, IL, May-June, pp. 52-66.

Naik *et al.* (2011): Naik, T. R., Kraus, R. N., Kumar, R., "Influence of Types of Coarse Aggregates on the Coefficient of Thermal Expansion of Concrete," *Journal of Materials in Civil Engineering*, American Society of Civil Engineers, Reston, VA, V. 23, No. 4, Apr., pp. 467-472.

PCI Bridge Committee (1978): "Tentative Design and Construction Specifications for Bridge Deck Panels," *PCI Journal*, Precast/Prestressed Concrete Insitute, Chicago, IL, V. 23, No. 1, pp. 32-39.

PCI (2006): *Manual for the Evaluation and Repair of Precast, Prestressed Concrete Bridge Products*, Precast/Prestressed Concrete Insitute, Chicago, IL.

Ross Bryan Associates, Inc. (1988): "Recommended Practice for Precast Prestressed Concrete Composite Bridge Deck Panels," *PCI Journal*, Precast/Prestressed Concrete Insitute, Chicago, IL, pp. 67-109.

Stocker *et al.* (1970): Stocker, M. F., and Sozen, M. A., "Investigation of Prestressed Concrete for Highway Bridges, Part V: Bond Characteristics of Prestressing Strand," The University of Illinois, Champaign, IL.

Tadros *et al.* (2003): Tadros, M. K., Nabil, A., Seguirant, A. J., and Gallt, J. G., *NCHRP Report 496: Prestress Losses in Pretensioned High-Strength Concrete Bridge Girders*, Transportation Research Board, Washington, D.C.

Tepfers (1973): Tepfers, R., "A Theory of Bond applied to Overlapped Tensile Reinforcement Splices for Deformed Bars," Chalmers University of Technology, Gotenborg, Sweden.

Texas Transportation Institute, and Texas Highway Department (1975): "Investigation to Determine Feasibility of Using In-Place Precast Prestressed Form Panels for Highway Bridge Decks," *PCI Journal*, Precast/Prestressed Concrete Insitute, Chicago, IL, V. 20, No. 3, May-June, pp. 62-67.

TxDOT (2011): *Bridge Design Manual*, Texas Department of Transportation, Austin, TX.

TxDOT (2004): *Standard Specifications for Construction and Maintenance of Highways, Streets, and Bridges*, Texas Department of Transportation, Austin, TX.

TxDOT 6348 (2010): “Project No. 0-6348 Controlling Cracking in Prestressed Concrete Panels and Optimizing Bridge Deck Reinforcing Steel,” The University of Texas at Austin, Austin, TX.

Zia *et al.* (1977): Zia, P., and Mostafa, T., "Development Length of Prestressing Strands," *PCI Journal*, Precast/Prestressed Concrete Insitute, Chicago, IL, V. 22, No. 5, Sep.-Oct., pp. 54-65.

Zia *et al.* (1979): Zia, P., Preston, H. K., Scott, N. L., and Workman, E. B., "Estimating Prestress Loss," *Concrete International Design and Construction*, American Concrete Institute, Farmington Hills, MI, V. 1, No. 6, June, pp. 32-38.